ELSEVIER

Physica D 124 (1998) 23–57

PHYSICA D

Spectral, diffusive and convective properties of fractal and spiral fields

J.R. Angilella, J.C. Vassilicos *

Department of Applied Mathematics and Theoretical Physics, University of Cambridge, Cambridge CB3 9EW, UK

Received 15 September 1997; received in revised form 3 March 1998
Communicated by U. Frisch

Abstract

Spectral, diffusive and convective properties of one-dimensional pulse fields displaying a well-defined Kolmogorov capacity $D \in [0, 1[$ are investigated.

The energy spectrum of fractal or spiral alternating pulse fields scales as k^D. The energy spectrum of homogeneous fractal non-alternating pulse fields scales as k^{-D}. Both these scaling laws hold in a range of wavenumbers between η^{-1} and L^{-1}, where η is the smallest distance between pulses and L ($\gg \eta$) is a characteristic large scale of the structure. The space-filling geometry, which is quantified by the Kolmogorov capacity D, makes the field less autocorrelated (more singular) in the alternating case, whereas it makes it more autocorrelated (less singular) in the non-alternating case.

Significant quantitative differences between the spectral properties of homogeneous fractals and of spirals exist. The energy spectrum of a spiral non-alternating pulse field scales as k^{-1} between x_N^{-1} and L^{-1}, where $x_N \sim \eta(L/\eta)^D \gg \eta$ characterizes the inhomogeneity of the structure. The spectrum is flat outside this wavenumber range.

When submitted to the action of molecular diffusion (molecular diffusivity ν) the energy of these fields decays as follows. Energy decay is accelerated in the case of fractal or spiral alternating pulse fields:

$$E(t) \sim \left(\frac{\sqrt{\nu t}}{\eta}\right)^{-1-D} \quad \text{for } \frac{\eta^2}{\nu} \ll t \ll \frac{L^2}{\nu},$$

and is delayed ("trapped") in the case of non-alternating homogeneous fractal pulse fields:

$$E(t) \sim \left(\frac{\sqrt{\nu t}}{\eta}\right)^{-1+D} \quad \text{for } \frac{\eta^2}{\nu} \ll t \ll \frac{L^2}{\nu}.$$

This energy trapping manifests itself in a different manner in the case of spiral non-alternating pulse fields. In this case energy decays only logarithmically for $\eta^2/\nu \ll t \ll x_N^2/\nu$, then decays like $t^{-1/2}$ for longer times.

When submitted to the combined action of convection and diffusion (Burgers equation) the energy of these fields of N pulses each of integral $m \gg \nu$ decays as follows. It is independent of D in the case of alternating pulse fields, and is delayed in the case of non-alternating pulse fields. For homogeneous fractal non-alternating pulse fields energy decays as

$$E(t) \sim \left(\frac{mt}{\eta^2}\right)^{-(D-1)/(D-2)} \quad \text{for } \frac{\eta^2}{m} \ll t \ll \frac{L^2}{Nm}.$$

* Corresponding author. Tel.: +44 1223 339868; fax: +44 1223 337918; e-mail: jcvio@damtp.cam.ac.uk

PII: S0167-2789(98)00162-6

For spiral non-alternating pulse fields energy decays as $t^{-1/2}$ for $x_N^2/Nm \ll t \ll L^2/Nm$, and the decay is much slower for $t \ll x_N^2/Nm$. This delay of energy decay is due to an anomalous collision rate between shocks which manifests itself differently according to whether the structure is homogeneous or not.

1. Introduction

Fields with a fractal or spiral geometry can have a power-law spectral signature with a non-integer exponent. Lundgren [13], in the framework of turbulence, pointed out that time-averaged strained spiral vortices have a $k^{-5/3}$ energy spectrum, and Moffatt [14] and Gilbert [8] showed that rolled-up scalar patches also display a spectrum with a non-integer exponent. Vassilicos and Hunt [20] generalized these results by showing that both fractal and spiral objects can have a well-defined Kolmogorov capacity, and that scalar fields displaying a sharp interface with well-defined Kolmogorov capacity have a power law energy spectrum the exponent of which depends on that capacity. In particular, it is observed that the larger the Kolmogorov capacity, the less steep the energy spectrum, so that the space-filling properties of these fields make them more singular. For example, a one-dimensional signal displaying an isolated discontinuity is known to have a k^{-2} energy spectrum for large wavenumbers k, whereas a on–off signal with discontinuities distributed in a fractal or spiral manner, with Kolmogorov capacity $D \in [0, 1[$, has a k^{D-2} energy spectrum for large wavenumbers [20]. This result is remarkable in that fractal and spiral distributions of discontinuities have identical spectral signatures, even if the scale-invariant properties of these two objects are qualitatively different. When submitted to a diffusive process, such fields have been shown to have remarkable properties due to the accumulation of their gradients [6,19]. Mainly, the energy decay of fractal or spiral distributions of discontinuities is faster than the energy decay of an isolated discontinuity. Here also, both fractals and spirals have the same diffusive properties.

In this paper we study the effects of the fractal or spiral structure of a field of *pulses* (rather than discontinuities) on its evolution under either the linear diffusion equation

$$\frac{\partial u}{\partial t} = \nu \frac{\partial^2 u}{\partial x^2}, \tag{1}$$

or the nonlinear diffusion equation

$$\frac{\partial u}{\partial t} + u\frac{\partial u}{\partial x} = \nu \frac{\partial^2 u}{\partial x^2}, \tag{2}$$

also called Burgers equation [3]. The quantity ν represents a molecular diffusivity or a kinematic viscosity.

There exists an enormous variety of quantitatively different fractal and spiral fields. The studies of Moffatt [14], Gilbert [8], Vassilicos and Hunt [20], Vassilicos [19] and Flohr and Vassilicos [6] concern fractal and spiral on–off fields. In this paper we study one-dimensional fields consisting of a number N of pulses on a fractal or spiral set. These fields are expressed in terms of delta functions as follows:

$$u_0(x) = \sum_{i=1}^{N} m_i \delta(x - x_i), \tag{3}$$

where x_i are points of a fractal or spiral set on a one-dimensional axis, and m_i is the spatial integral of the pulse located at x_i. The one-dimensional spiral sets of points we consider in this paper are such that $x_i \sim i^{-\alpha} (\alpha > 0)$, and correspond to a cut through a two-dimensional algebraic spiral of equation $\rho \sim \phi^{-\alpha}$ in polar coordinates (ρ, ϕ). The subscript 0 in Eq. (3) is used because in this paper we study the solutions of Eqs. (1) and (2) with initial conditions $u_0(x)$ given by (3).

The fractal or spiral property of the set of points x_i is quantitatively introduced by assuming that the minimum number of segments of size r required to cover all the points x_i depends on r as follows:

$$N_{\text{boxes}}(r) \sim N \quad \text{for } r < \eta, \tag{4}$$

$$N_{\text{boxes}}(r) \sim N\left(\frac{r}{\eta}\right)^{-D} \sim \left(\frac{r}{L}\right)^{-D} \quad \text{for } \eta \ll r \ll L, \tag{5}$$

$$N_{\text{boxes}}(r) \sim 1 \quad \text{for } L < r, \tag{6}$$

where $D \in [0, 1[$ is the Kolmogorov capacity of the set of points, N is the total number of points, η is the smallest separation between points and L is the overall length scale of the structure. In this paper we assume $\eta \ll L$. The closer D is to 1 the more space-filling is the set of points x_i. Note also that the total number of points is such that $N \sim (L/\eta)^D$ and therefore increases with L/η in a way determined by D.

It may be worth mentioning at this stage that the Hopf–Cole transformation [4,11]

$$\theta(x,t) = \exp\left(-\frac{1}{2\nu}\int^{x} u(x,t)\,\mathrm{d}x\right), \tag{7}$$

$$u(x,t) = -2\nu\frac{\partial}{\partial x}\log(\theta) \tag{8}$$

transforms the Burgers equation (2) into a linear diffusion equation for the Hopf–Cole variable θ:

$$\frac{\partial\theta}{\partial t} = \nu\frac{\partial^2\theta}{\partial x^2}, \tag{9}$$

and that we are particularly interested in determining the energy decay, correlation length and diffusive length-scale of fractal and spiral fields evolving under the action of either the linear diffusion equation or the nonlinear Burgers equation. The energy of a field that is evolving under the action of a linear diffusion equation is given by

$$E(t) = \int_0^{+\infty} E(k,t)\,\mathrm{d}k, \tag{10}$$

where

$$E(k,t) = E_0(k)\mathrm{e}^{-2\nu k^2 t},$$

and $E_0(k)$ is the energy spectrum of the initial fractal or spiral field. The diffusive length-scale $\delta(t)$ [19] is defined on the basis of the correlation length $\mathcal{L}(t)$ which is given by the weighted average

$$\mathcal{L}(t) = \int k^{-1}\frac{E(k,t)}{E(t)}\,\mathrm{d}k. \tag{11}$$

Hence, in the case of linear diffusive decay, the time-dependencies of $E(t)$, $\mathcal{L}(t)$ and $\delta(t)$ can all be readily calculated provided that the energy spectrum $E_0(k)$ of the initial fractal or spiral field is known. In Section 2 we derive the energy spectra of two qualitatively different types of fractal or spiral pulse fields (3), and in Section 3 we spell out the consequences of these initial energy spectra for the decay of these fractal or spiral pulse fields by linear diffusion. We find that differences in the signs of pulses in the initial fractal or spiral pulse field (3) lead to dramatic qualitative differences in the nature of the decay, in one case (Fig. 1(b)) an acceleration of diffusion, in another case (Fig. 1(a)) a deceleration of diffusion and trapping of energy by the fractal or spiral structure. Also,

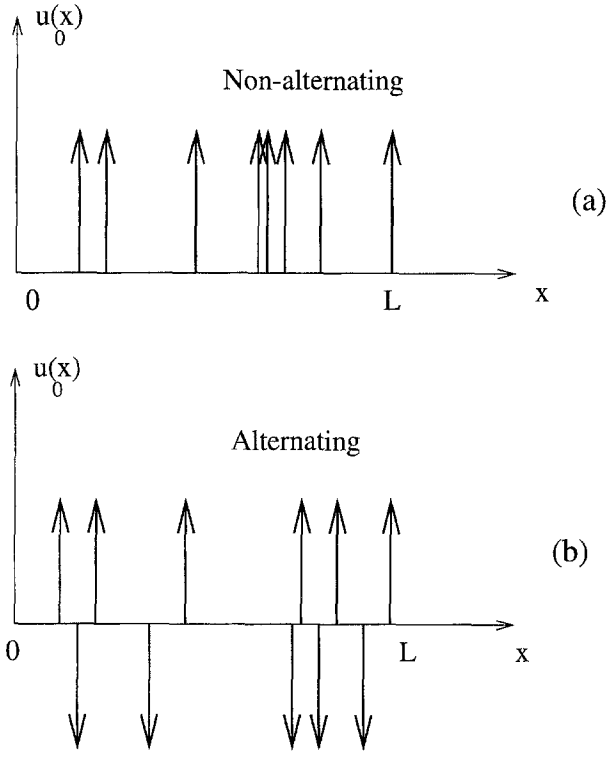

Fig. 1. Sketch of the field $u_0(x)$. Vertical arrows denote δ functions.

in contrast with the decay of fractal and spiral on–off fields, we find differences in the ways that fractal and spiral pulse fields decay.

Following Gurbatov and Crighton [9], Section 4 is devoted to the analysis of the Burgers equation with initial data given by (3). We are particularly interested in deriving the convective properties of the field $u_0(x)$ from the diffusive properties of its Hopf–Cole transformed field $\theta_0(x)$. Indeed, in the limit of vanishing viscosity and for t sufficiently large, the field $u(x,t)$ is characterized by triangular shocks moving on the x-axis, and likely to collide [12,17]. The rate of energy decay of the field $u(x,t)$ strongly depends on the frequency of these collisions, which are known to delay the energy decay [12,17]. These strongly nonlinear events (shock formations, displacement and collisions) correspond to linear events in the Hopf–Cole transformed field $\theta(x,t)$, and in the case of the field u_0 given by (3), $\theta_0(x)$ also has fractal or spiral properties similar to those of u_0. We observe that these geometrical properties can lead to remarkable diffusive properties in $\theta(x,t)$, and therefore to remarkable convective properties in the field $u(x,t)$.

2. The energy spectra of fractal and spiral pulse fields

The two cases of fractal or spiral fields (3) that we consider are:
- *the alternating case*: $m_i = (-1)^{i+1}m$ for all i,
- *the non-alternating case*: $m_i = m$ for all i.

Examples of fields $u_0(x)$ in the alternating and the non-alternating cases are shown in Fig. 1.

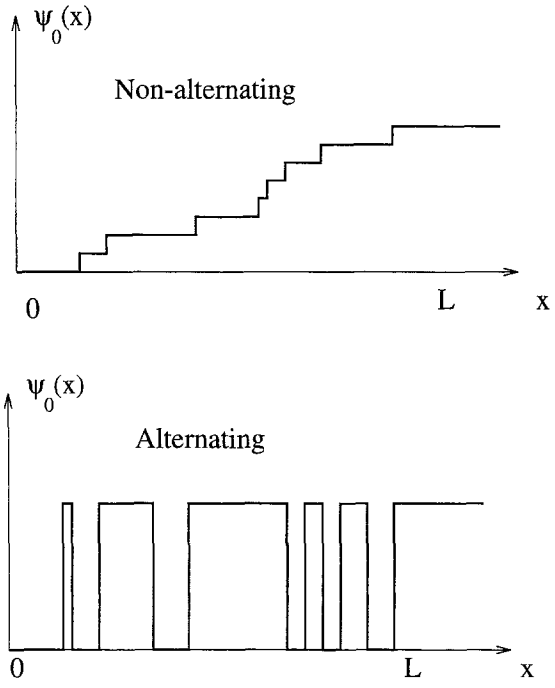

Fig. 2. Sketch of the initial velocity potential, $\psi_0(x) = \int_0^x u_0(x)\,\mathrm{d}x$. In the alternating case $\psi_0(x)$ is a on–off function. In the non-alternating case it is a step function, and is often referred to as Devil staircase when the discontinuity points are located on a Cantor set.

We calculate the energy spectrum $E_0(k)$ of $u_0(x)$ in two steps. Firstly, we calculate the energy spectrum $E_{\psi 0}(k)$ of the potential $\psi_0(x) = \int_0^x u_0(x)\,\mathrm{d}x$ (Fig. 2) and secondly we derive $E_0(k)$ from $E_{\psi 0}(k)$ by using $E_0(k) = k^2 E_{\psi 0}(k)$. The points x_i are discontinuity points of $\psi_0(x)$ and will hereinafter be referred to as such.

In the alternating case $E_{\psi 0}(k)$ has been obtained by Vassilicos and Hunt [20] and their result implies that (see Appendix A for $E_0(k)$ where $k \ll 1/L$)

$$E_0(k) \sim \frac{m^2}{L}(N \text{ odd}) \quad \text{or} \quad \frac{m^2}{L}(kL)^2(N \text{ even}), \quad k \ll 1/L, \tag{12}$$

$$E_0(k) \sim \frac{m^2}{L}(kL)^D, \quad \frac{1}{L} \ll k \ll \frac{1}{\eta}, \tag{13}$$

$$E_0(k) \sim \frac{m^2}{L}N, \quad \frac{1}{\eta} \ll k, \tag{14}$$

both for fractal and spiral fields indiscriminately, under the sole condition that (4)–(6) are valid.

In the non-alternating case we first calculate the structure function

$$\langle \delta\psi_0^2(r)\rangle = \langle(\psi_0(x+r) - \psi_0(x))^2\rangle = 2\langle\psi_0(x)^2\rangle - 2\langle\psi_0(x+r)\psi_0(x)\rangle,$$

where the brackets $\langle\cdot\rangle$ denote a spatial average, and then derive $E_{\psi 0}(k)$ by operating a Fourier transform [1] on $\langle\psi_0(x+r)\psi_0(x)\rangle$.

[1] To avoid trivial averages in the non-alternating case, the spatial average is calculated over a finite domain of size L containing all points $x_1, \ldots, x_N$. This definition of a spatial average, and therefore of $\langle\psi_0(x)\psi_0(x+r)\rangle$ and $\langle u_0(x)u_0(x+r)\rangle$, leaves the relation $E_0(k) = k^2 E_{\psi 0}(k)$ unaffected in the limit $k \gg 1/L$. Note that this truncation is also responsible for the behaviour of $\langle\delta\psi_0^2(r)\rangle$ for r close to L (Figs. 3 and 6).

For a given distance r we observe that $\psi(x+r)-\psi_0(x) = mq(x,r)$, where $q(x,r)$ is the number of discontinuity points lying in the segment $[x, x+r]$. Hence,

$$\langle \delta\psi_0^2(r)\rangle = m^2 \frac{1}{L} \int_{-\infty}^{+\infty} q(x,r)^2 \,\mathrm{d}x. \tag{15}$$

This relation is now used to derive $\langle \delta\psi_0^2(r)\rangle$ and then $E_{\psi 0}(k)$. It turns out that the results are markedly different for homogeneous fractals and for spirals, in distinct contrast with the alternating case where fractal and spiral pulse fields have the same spectra. This difference stems from the sensitivity of the spectrum in the non-alternating case to the degree of fractal homogeneity of the set of discontinuity points, and spiral sets may be viewed as an extreme case of fractal non-homogeneity. In Section 2.1 we calculate the energy spectrum of homogeneous fractal non-alternating pulse fields. In Section 2.2 we calculate the energy spectrum of spiral non-alternating pulse fields.

2.1. Energy spectrum of homogeneous fractal non-alternating pulse fields

Given the minimum number of segments of size r needed to cover all the points of a set, this set of points is a homogeneous fractal when the number of points $\bar{q}(r)$ lying in any one of the segments of this minimal coverage is the same for all these segments (see [10]). Hence, for a homogeneous fractal set of points we must have

$$\bar{q}(r) \simeq \frac{N}{N_{\mathrm{boxes}}(r)}. \tag{16}$$

The Cantor set is an example of a homogeneous fractal (see Appendix B).

For a set of discontinuity points that is homogeneous fractal, the dependence of $q(x,r)$ on x is characterized by regions of high activity with a peak value of $\bar{q}(r)$ interspersed between regions of low activity where $q(x,r) \simeq 0$. The number of regions of high activity is given by $N_{\mathrm{boxes}}(r)$ and the integral in Eq. (15) can therefore be approximated as follows (see [15]):

$$\int_{-\infty}^{+\infty} q(x,r)^2 \,\mathrm{d}x \simeq \sum_{\mathrm{boxes}} r\bar{q}(r)^2 = r\bar{q}(r)^2 N_{\mathrm{boxes}}(r) \simeq r\frac{N^2}{N_{\mathrm{boxes}}(r)}, \tag{17}$$

where $\sum_{\mathrm{boxes}}$ denotes a sum over the minimal number of segments of size r that is needed to cover the set of discontinuity points. Hence, by making use of (4)–(6) we obtain

$$\langle \delta\psi_0^2(r)\rangle \sim m^2 \frac{r}{L} N \quad \text{for } r < \eta, \tag{18}$$

$$\langle \delta\psi_0^2(r)\rangle \sim m^2 N^2 \left(\frac{r}{L}\right)^{1+D} \quad \text{for } \eta \ll r \ll L, \tag{19}$$

$$\langle \delta\psi_0^2(r)\rangle \sim m^2 \frac{r}{L} N^2 \quad \text{for } L < r. \tag{20}$$

This result can also be obtained by a different approach based on a statistical method which we present in Appendix C. Furthermore, the result can be generalized to structure functions of order $p \geq 2$, and in the range $\eta \ll r \ll L$ we have $\langle \delta\psi_0^p(r)\rangle \sim m^p N^p (r/L)^{1+(p-1)D}$. Numerical calculations of the structure function $\langle \delta\psi_0^2(r)\rangle$ are in good agreement with (18) and (19). An example of such numerical agreement is shown in Fig. 3 where the numerically calculated structure function $\langle \delta\psi_0^2(r)\rangle$ is plotted for a triadic Cantor set of discontinuity points, together with prediction (18) and (19) for comparison.

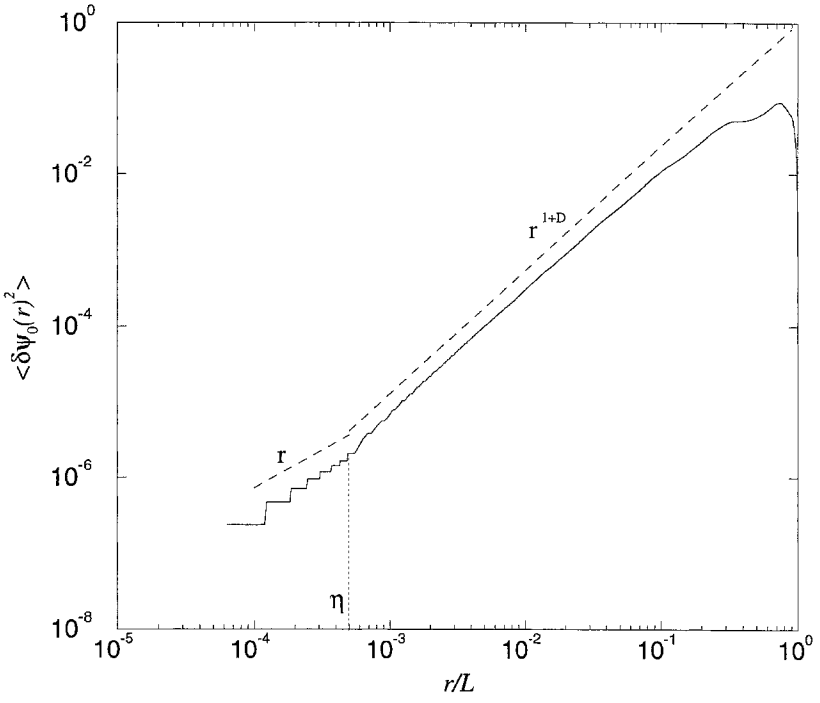

Fig. 3. Structure function of the velocity potential $\langle \delta\psi_0(r)^2 \rangle$, in the non-alternating case, for discontinuity points displayed on a triadic Cantor set ($D = \ln 2/\ln 3 \simeq 0.63$). Dashed lines show the theoretical predictions (18) and (19).

By a Fourier transformation of the autocorrelation function stemming from (18) – (20) we obtain $E_{\psi 0}(k)$ which we multiply by k^2 to get

$$E_0(k) \sim \frac{m^2}{L} N^2, \quad k \ll \frac{1}{L}, \tag{21}$$

$$E_0(k) \sim \frac{m^2}{L} N^2 (kL)^{-D}, \quad \frac{1}{L} \ll k \ll \frac{1}{\eta}, \tag{22}$$

$$E_0(k) \sim \frac{m^2}{L} N, \quad \frac{1}{\eta} \ll k. \tag{23}$$

We therefore obtain that $E_0(k) \sim L\langle u_0 \rangle^2 \sim m^2 N^2 / L$ for wavelengths much larger than the overall length-scale of the structure. For wavelengths smaller than the finest scale of the structure the spectrum is also constant, but its value $m^2 N/L$ as opposed to $m^2 N^2/L$ can be thought of as resulting from a random walk effect (see Appendix D). In Fig. 4 we plot the running averages of a numerically calculated Fourier spectrum of a fractal non-alternating pulse field which exhibit good agreement with our analytical prediction (22). Fig. 5 shows the corresponding wavelet spectrum, which can be shown to scale like the Fourier spectrum (Appendix E), but which is more smooth than the Fourier spectrum, due to the smoothing effect of the convolution operation in the wavelet transform. The wavelet we use is the second derivative of the gaussian ("mexican hat").

Comparing Eqs. (12)–(14) with Eqs. (21)–(23) we see that the difference between the spectra of alternating and non-alternating pulse fields is dramatic. In the range $1/L \ll k \ll 1/\eta$, $E_0(k) \sim k^D$ for fractal (in particular homogeneous fractal) alternating pulse fields, whereas $E_0(k) \sim k^{-D}$ for homogeneous fractal non-alternating pulse fields. Hence, for a given Kolmogorov capacity D, a homogeneous fractal structure consisting of non-alternating

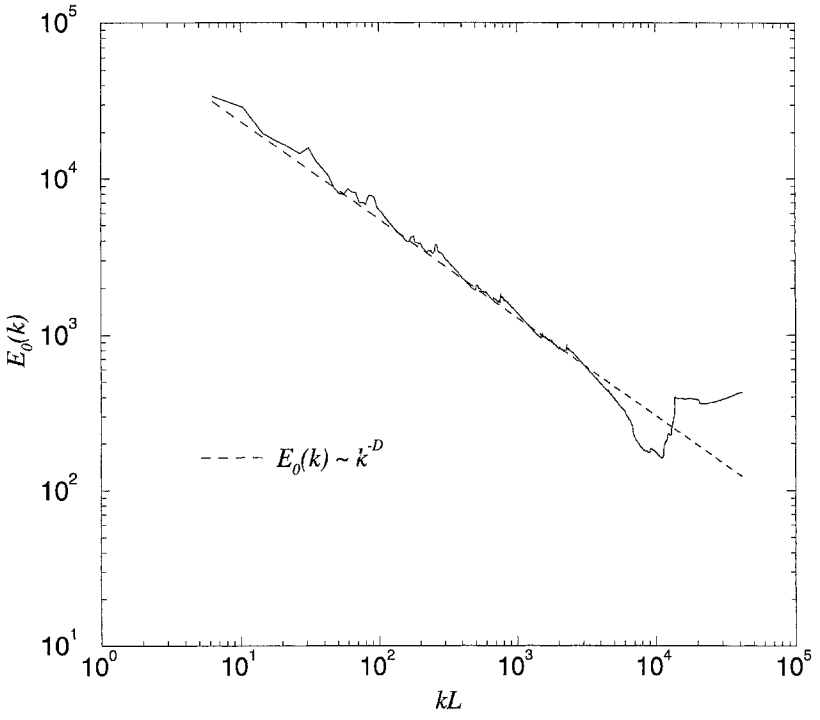

Fig. 4. Running averages of the energy spectrum of the fractal velocity field $u(x)$ in the non-alternating case. Discontinuity points are positioned on a triadic Cantor set ($D = \ln 2/\ln 3 \simeq 0.63$).

pulses is less singular than an isolated pulse, whereas a fractal structure consisting of alternating pulses is more singular than an isolated pulse. Furthermore, as D increases, fractal alternating pulse fields become more singular and therefore less autocorrelated, whereas homogeneous fractal non-alternating pulse fields become less singular and therefore more autocorrelated.

Unlike the spectra of alternating pulse fields which are the same for fractal and spiral sets, the spectra of non-alternating pulse fields are not the same for homogeneous fractal sets and for spiral sets. In the following section we calculate the energy spectrum of spiral non-alternating pulse fields.

2.2. *Energy spectrum of spiral non-alternating pulse fields*

A canonical example of a spiral set of points for which (4)–(6) are valid with a well-defined Kolmogorov capacity $D \in]0, 1[$ is the algebraic spiral set of points x_i defined by

$$x_i = Li^{-\alpha}, \tag{24}$$

where $\alpha > 0$ and $i = 1, 2, 3, \ldots$. Because there are N such points, the smallest separation between points of the spiral set is $\eta = x_{N-1} - x_N \simeq L\alpha N^{-\alpha-1}$ and $D = 1/(\alpha + 1)$ in the range of length-scales between η and $x_1 - x_2 = L(1 - 2^{-\alpha})$ [20]. Note that in the limit $\eta \ll L(1 - 2^{-\alpha})$ (which therefore implies that $\eta \ll \alpha L$ since $\alpha > 1 - 2^{-\alpha}$),

$$N \simeq \left(\frac{\alpha L}{\eta}\right)^D. \tag{25}$$

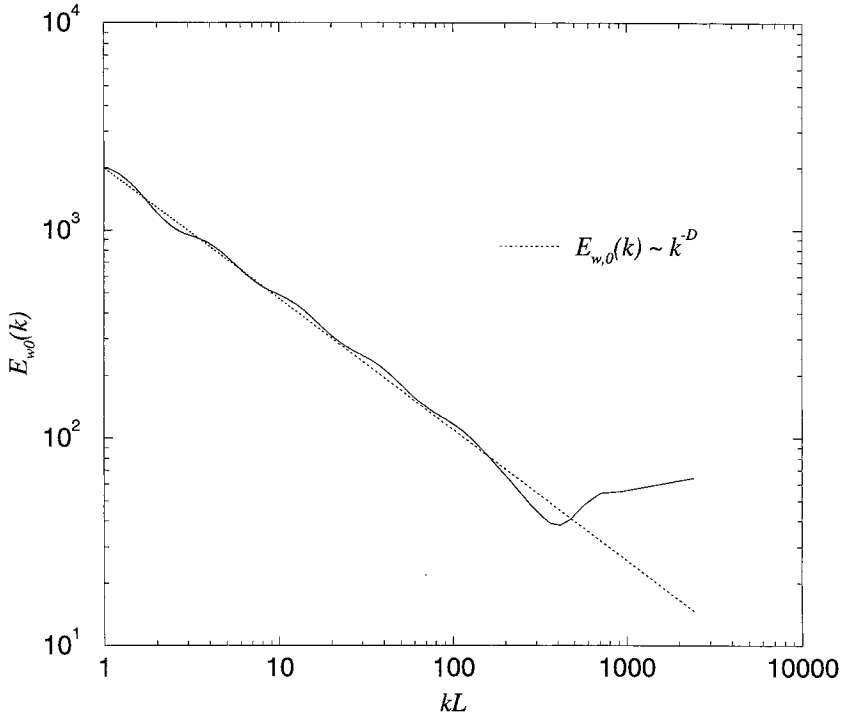

Fig. 5. Wavelet energy spectrum E_{w0} (see Appendix E) of the fractal velocity field $u_0(x)$ in the non-alternating case. Discontinuity points are positioned on a triadic Cantor set. The wavelet transform of u_0 has been squared and integrated over all positions x to obtain $E_{w0}(l)$ (see Appendix E), where l denotes the scale parameter. We plot $E_{w0}(k)(\equiv E_{w0}(l)$ for $k = 1/l)$ versus $kL = L/l$ (in Fig. 4 we plot the Fourier spectrum $E_0(k)$ versus $kL = 2\pi L/l$). Due to the smoothing effect of the convolution operator the wavelet spectrum is less irregular than the corresponding Fourier spectrum.

We calculate the energy spectrum $E_0(k)$ of a field $u_0(x)$ consisting of non-alternating pulses that are positioned on this spiral set of points x_i. Again, we first calculate the structure function $\langle \delta\psi_0^2(r)\rangle$ from which we deduce $E_{\psi 0}(k)$ and then $E_0(k) = k^2 E_{\psi 0}(k)$. We do not use the assumption of fractal homogeneity here; in fact the spiral may be viewed as an extreme case of fractal non-homogeneity. We now proceed with the calculation which leads to results (37)–(42).

When $r < \eta$, segments of size r either cover one discontinuity point or none, but nowhere more than one. Because there are exactly N discontinuity points, $\int_{-\infty}^{+\infty} q(x,r)^2\,\mathrm{d}x = rN$, and from (15) it follows that

$$\langle \delta\psi_0^2(r)\rangle = m^2 \frac{r}{L} N \quad \text{for } r < \eta, \tag{26}$$

which is identical to the result (18) in the fractal non-alternating case.

To calculate $\langle \delta\psi_0^2(r)\rangle$ for $r \gg \eta$ we notice that $q(x,r) = 0$ outside $]x_N - r, L[$ and split the space integration in (15) in the following three parts:

$$\int_{-\infty}^{+\infty} q(x,r)^2\,\mathrm{d}x = \underbrace{\int_{x_N - r}^{x_N} q(x,r)^2\,\mathrm{d}x}_{T_1(r)} + \underbrace{\int_{x_N}^{x_{N_c}} q(x,r)^2\,\mathrm{d}x}_{T_2(r)} + \underbrace{\int_{x_{N_c}}^{L} q(x,r)^2\,\mathrm{d}x}_{T_3(r)},$$

where $N_c = N_c(r)$ is defined such that $r = x_{N_c} - x_{N_c+1}$. This definition is possible because $\eta \ll r$, and if $N_c(r)$ is large enough,

$$N_c(r) \simeq \left(\frac{\alpha L}{r}\right)^{1/(\alpha+1)} = \left(\frac{\alpha L}{r}\right)^{D}, \tag{27}$$

which is valid in the range $\eta \ll r \ll \alpha L$.

The term $T_3(r)$ is readily calculated if we notice that in the region of space $x_{N_c} < x < L$, segments of size r cannot cover more than one discontinuity point and therefore $q(x,r) = 1$ where there is a discontinuity point between x and $x + r$ and $q(x,r) = 0$ where there is no such point between x and $x + r$. Because there are N_c discontinuity points between x_{N_c} and L,

$$T_3(r) \simeq r N_c(r) \simeq \alpha L \left(\frac{r}{\alpha L}\right)^{1-D} \tag{28}$$

in the range $\eta \ll r \ll \alpha L$.

To calculate $T_2(r)$ we write

$$T_2(r) = \sum_{i=N_c+1}^{N} \int_{x_i}^{x_{i-1}} q(x,r)^2 \, \mathrm{d}x,$$

and because $q(x,r) = i - n_i(r)$ with $x_{n_i} \simeq x_i + r$ for $x \in]x_i, x_{i-1}[$,

$$T_2(r) \simeq \sum_{i=N_c+1}^{N} (x_{i-1} - x_i)(i - n_i)^2 \tag{29}$$

with

$$n_i \simeq \left(i^{-\alpha} + \frac{r}{L}\right)^{-1/\alpha}. \tag{30}$$

In the limit where $r \ll \alpha L$, N_c is much larger than 1 and $x_{i-1} - x_i \simeq \alpha L i^{-\alpha-1}$ for $i > N_c$. Moreover, if $(r/L)i^{\alpha} \ll 1$ for all $i \leq N$, a condition that is satisfied when $r \ll x_N$, we have

$$q(x,r) = i - n_i(r) \simeq \frac{r}{\alpha L} i^{\alpha+1}. \tag{31}$$

It follows that

$$T_2(r) \simeq \alpha L \sum_{i=N_c+1}^{N} i^{1-\alpha} \left(\frac{r}{\alpha L} i^{\alpha}\right)^2. \tag{32}$$

The sum in (32) can be replaced by an integral, and we therefore obtain

$$T_2(r) \simeq \frac{\alpha L}{\alpha + 2} \left(\frac{r}{\alpha L}\right)^2 N^{2+\alpha} \quad \text{for } \eta \ll r \ll x_N, \tag{33}$$

where the upper limit of the range is x_N because $x_N \ll \alpha L$ in the limit $\eta \ll \alpha L$. In Appendix F we calculate $T_2(r)$ in the range $x_N \ll r \ll \alpha L$ and find that $T_2 \ll T_1$ in that range.

To calculate $T_1(r)$ we write

$$T_1(r) = \sum_{i=n_N+1}^{N} \int_{x_i}^{x_{i-1}} q(x,r)^2 \, \mathrm{d}x,$$

which implies

$$T_1(r) \simeq \sum_{i=n_N+1}^{N} (x_{i-1} - x_i)(N+1-i)^2. \tag{34}$$

Note that $n_N = n_N(r) \simeq (N^{-\alpha} + r/L)^{-1/\alpha}$ and $T_1(r)$ can further be approximated by

$$T_1(r) \simeq \alpha L \sum_{i=n_N+1}^{N} i^{-1-\alpha}(N+1-i)^2. \tag{35}$$

The sum in (35) can be replaced by an integral, and in the limit where $x_N \ll r$ (and therefore $n_N \ll N$) the dominant contribution to $T_1(r)$ turns out to be

$$T_1(r) \simeq N^2 r \quad \text{for } x_N \ll r \ll \alpha L. \tag{36}$$

In Appendix F we show that in the limit where $\eta \ll \alpha L$, $T_2 \gg T_1, T_3$ in the range $\eta \ll r \ll x_N$ and $T_1 \gg T_2, T_3$ in the range $x_N \ll r \ll \alpha L$. Hence, from (26), (33) and (36):

$$\langle \delta\psi_0^2(r) \rangle \simeq m^2 \frac{r}{L} N \quad \text{for } r < \eta, \tag{37}$$

$$\langle \delta\psi_0^2(r) \rangle \simeq \frac{m^2}{\alpha(\alpha+2)} N^{2+\alpha} \left(\frac{r}{L}\right)^2 \quad \text{for } \eta \ll r \ll x_N, \tag{38}$$

$$\langle \delta\psi_0^2(r) \rangle \simeq m^2 \frac{r}{L} N^2 \quad \text{for } x_N \ll r \ll \alpha L. \tag{39}$$

Numerical calculations of the structure function $\langle \delta\psi_0^2(r) \rangle$ are in good agreement with (37)–(39). An example of such numerical agreement is shown in Fig. 6.

The energy spectrum $E_0(k)$ of the spiral non-alternating pulse field can now be deduced:

$$E_0(k) \sim \frac{m^2}{L} N^2, \quad \frac{1}{(\alpha L)} \ll k \ll \frac{1}{x_N}, \tag{40}$$

$$E_0(k) \sim \frac{m^2}{L} N^{2+\alpha} (kL)^{-1}, \quad \frac{1}{x_N} \ll k \ll \frac{1}{\eta}, \tag{41}$$

$$E_0(k) \sim \frac{m^2}{L} N, \quad \frac{1}{\eta} \ll k. \tag{42}$$

In Fig. 7 we plot numerically calculated spectra of spiral non-alternating pulse fields which exhibit good agreement with our analytical predictions.

Unlike the energy spectra of alternating pulse fields and of homogeneous fractal non-alternating pulse fields, the energy spectrum of spiral non-alternating pulse fields is not scale-invariant in the asymptotic wavenumber range $kL \to \infty$, $k\eta \to 0$. A characteristic length-scale exists between η and L which is x_N, and which represents the length-scale of non-homogeneity of the spiral pulse field. This is because the dependence on x and r of $q(x,r)$, the number of discontinuity points in $[x, x+r]$, is qualitatively different for $r \ll x_N$ and for $r \gg x_N$. This qualitative difference manifests itself in the above calculations at the stages where $n_i(r)$ (Eq. (30)) is linearized, leading to different expressions for T_2 and T_1 in the cases $r \ll x_N$ (Eqs. (33) and (F.1)) and $r \gg x_N$ (Eqs. (F.3) and (36)).

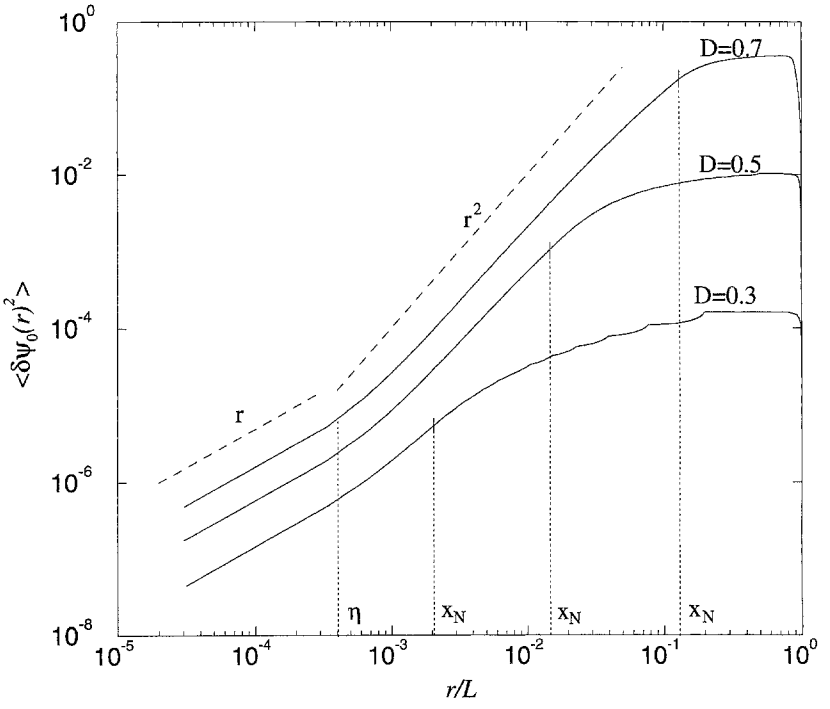

Fig. 6. Structure function of the velocity potential $\langle \delta\psi_0(r)^2 \rangle$ in the non-alternating case, for discontinuity points displayed on a spiral. The Kolmogorov capacity of each spiral is D. The scale $r = \eta$ is the same for the three spirals. The range of scales $\eta \ll r \ll x_N$ over which $\langle \delta\psi_0(r)^2 \rangle \sim r^2$ increases with D.

The energy spectra of alternating pulse fields are not sensitive to the fractal homogeneity or non-homogeneity of the field; their wavenumber dependence is uniquely determined by the Kolmogorov capacity D of the fractal or spiral set of discontinuity points x_i. However, the energy spectra of non-alternating pulse fields are sensitive to whether the field is homogeneously fractal or not. The energy spectrum (22) is obtained for a homogeneous fractal non-alternating pulse field, and the energy spectrum (40)–(42) is obtained for a spiral non-alternating pulse field. Spiral sets of points may be conceived as extreme cases of non-homogeneous fractals and the length-scale x_N is characteristic of this non-homogeneity.

Nevertheless, within the range $1/(\alpha L) \ll k \ll 1/\eta$, there exist two separate ranges of wavenumbers, where the energy spectrum is scale-invariant: the range $1/(\alpha L) \ll k \ll 1/x_N$, where $E_0(k)$ is independent of k and the range $1/x_N \ll k \ll 1/\eta$, where $E_0(k) \sim k^{-1}$. The scaling exponents of these scale-invariant spectra (respectively 0 and -1) do not depend on D but the ranges over which either scaling law is valid do depend on D. As D increases the range $1/x_N \ll k \ll 1/\eta$ increases at the expense of the range $1/(\alpha L) \ll k \ll 1/x_N$ which decreases. Hence, as D increases, it is the range over which $E_0(k) \sim k^{-1}$ that increases at the expense of the range over which $E_0(k)$ is independent of k. This means that the more space-filling the spiral, the less singular and therefore the more autocorrelated is the spiral non-alternating pulse field. A similar conclusion holds for homogeneous fractal non-alternating pulse fields but because of a qualitatively different reason; because the energy spectrum of homogeneous fractal non-alternating pulse fields steepens as D increases over a range of wavenumbers that is not affected by D.

Next, we use the energy spectra $E_0(k)$ obtained in this section to investigate the linear diffusive decay of fractal and spiral pulse fields, and in particular to calculate the time dependencies of their energy $E(t)$ and length-scales $\mathcal{L}(t)$ and $\delta(t)$ using Eqs. (10) and (11).

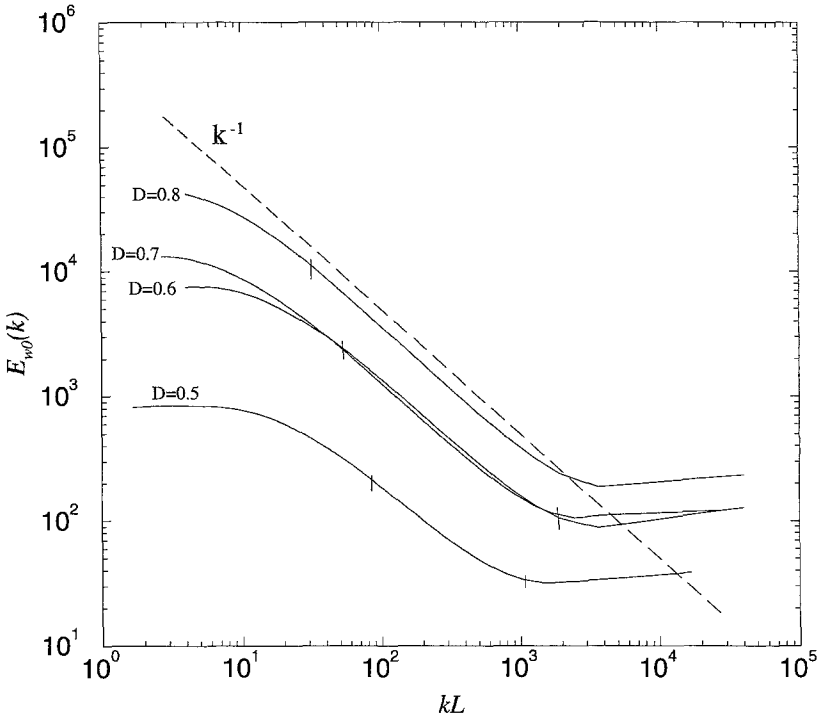

Fig. 7. Wavelet energy spectrum of $u_0(x)$ (see Appendix E) in the non-alternating case, for discontinuity points positioned on a spiral. Small vertical lines on each curve indicate the wavenumbers x_N^{-1} and $\eta^{-1}(> x_N^{-1})$. In agreement with the theory, no power law of the form k^{-D} is observed, but a k^{-1} power law is observed for all D. Note that the range of scales over which this power-law is valid increases with D.

3. Acceleration and deceleration of diffusion

For wavenumbers $k \gg 1/\eta$, the energy spectrum $E_0(k)$ is the same in all cases: it is $E_0(k) \sim (m^2/L)N$ for all pulse fields considered here, whether fractal or spiral, alternating or non-alternating. This high wavenumber part of the spectrum $E_0(k)$ determines the linear diffusive decay of pulse fields at very small time t, namely $0 < t \ll \eta^2/\nu$. For such short times, Eq. (10) simplifies to

$$E(t) \simeq \int_0^{1/\eta} E_0(k)\,\mathrm{d}k + \int_{1/\eta}^{+\infty} E_0(k)\mathrm{e}^{-2\nu k^2 t}\,\mathrm{d}k.$$

By setting $E_\eta = \int_0^{1/\eta} E_0(k)\,\mathrm{d}k$ (which approximates the energy of the signal at $t \simeq \eta^2/\nu$) and using $E_0(k) \sim (m^2/L)N$ for $k \gg 1/\eta$ we get

$$E(t) - E_\eta \sim \frac{m^2}{L} N(\nu t)^{-1/2} \left(\frac{\sqrt{\pi}}{2\sqrt{2}} + \mathrm{O}\left(\left(\frac{\nu t}{\eta} \right)^{1/2} \right) \right) \quad \text{for } 0 < t \ll \eta^2/\nu.$$

Hence for finite times t much shorter than η^2/ν, pulse fields, whether fractal, spiral, alternating or non-alternating, decay like isolated pulses and the value of $E(t) - E_\eta$ for a field of N pulses is simply N times the value of $E(t) - E_\eta$ for one isolated pulse.

For times $t \gg \eta^2/\nu$, the integral $\int_{1/\eta}^{+\infty} E_0(k)\mathrm{e}^{-2\nu k^2 t}\,\mathrm{d}k$ is negligible and (10) becomes

$$E(t) \simeq \int_0^{1/\eta} E_0(k)\mathrm{e}^{-2\nu k^2 t}\,\mathrm{d}k, \tag{43}$$

and in the intermediate time-range $\eta^2/\nu \ll t \ll L^2/\nu$, (43) can be approximated as follows:

$$E(t) \simeq \int_0^{1/L} E_0(k)\,\mathrm{d}k + \int_{1/L}^{1/\eta} E_0(k)\mathrm{e}^{-2\nu k^2 t}\,\mathrm{d}k \quad \text{for } \eta^2/\nu \ll t \ll L^2/\nu. \tag{44}$$

3.1. Linear diffusive decay of alternating pulse fields: accelerated diffusion

The energy spectrum $E_0(k)$ of alternating pulse fields, whether fractal or spiral, is given by (12)–(14). The first integral in Eq. (44) equals m^2/L^2 if N is odd and $\frac{1}{3}m^2/L^2$ if N is even. Hence,

$$E(t) \sim \frac{m^2}{L} + \frac{m^2}{L}\int_{1/L}^{1/\eta} (kL)^D \mathrm{e}^{-2\nu k^2 t}\,\mathrm{d}k$$

for times $L^2/\nu \gg t \gg \eta^2/\nu$. By writing the above integral in terms of the incomplete gamma function (see Appendix G), and by expanding it for $\sqrt{\nu t} \gg \eta$, we obtain

$$\frac{E(t)}{E_\eta} \sim \left(\frac{\sqrt{\nu t}}{\eta}\right)^{-1-D} + \mathrm{O}((\eta/L)^{1+D}) \quad \text{for } \frac{\eta^2}{\nu} \ll t \ll \frac{L^2}{\nu}, \tag{45}$$

where we have made use of $E_\eta \sim (m^2/L^2)(L/\eta)^{1+D}$. The term $\mathrm{O}((\eta/L)^{1+D})$ is negligible in front of $(\sqrt{\nu t}/\eta)^{-1-D}$ because $t \ll L^2/\nu$. The classical $t^{-1/2}$ result is recovered when $D = 0$, that is when the structure is either not fractal, not spiral or spiral with $D = 0$ (such as in the case of a logarithmic spiral, see [20]) The prediction (45) is confirmed numerically (see Fig. 8) by computing the energy of

$$u(x,t) = \sum_{i=1}^{N} \frac{m_i}{2\sqrt{\pi\nu t}} \mathrm{e}^{-(x-x_i)^2/4\nu t}, \tag{46}$$

which is the well-known solution of Eq. (1) with initial data given by (3), where $m_i = (-1)^{i+1}m$. From (45) we conclude that the more space-filling the set of points supporting the pulses, the larger the value of D and therefore the faster the decay of the alternating pulse field in the intermediate time-range $\eta^2/\nu \ll t \ll L^2/\nu$. This acceleration of diffusion by the fractal or spiral structure of the field has already been observed in on–off fields by Vassilicos [19] and in scalar fields evolving in a vortex by Flohr and Vassilicos [6].

We now show that non-alternating pulse fields have diametrically opposite diffusive properties: the space-filling property of non-alternating pulse fields has a decelerating rather than accelerating effect on diffusion. We also show that, unlike fractal and spiral alternating pulse fields, the diffusive properties of spiral and fractal non-alternating pulse fields are distinct.

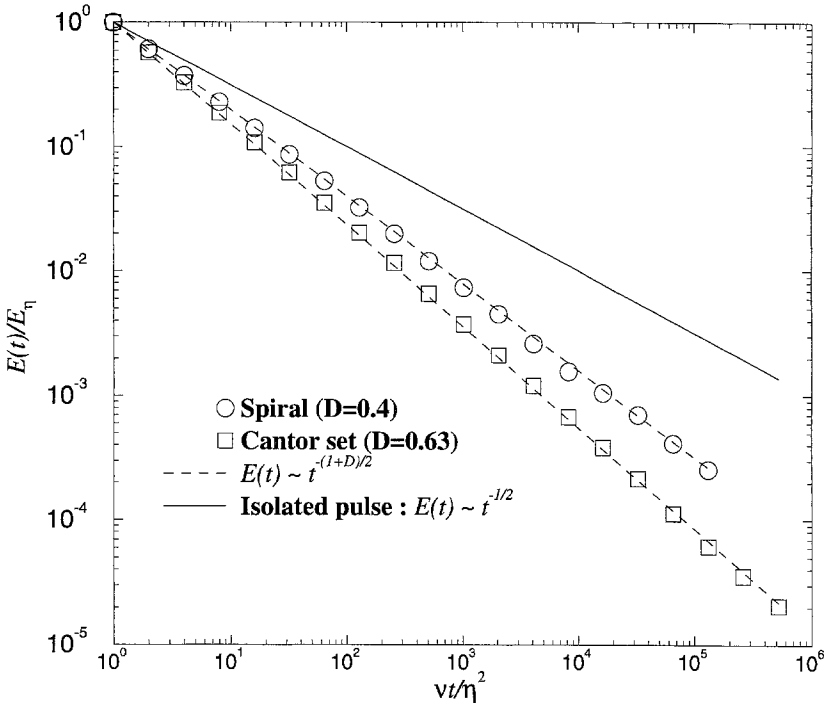

Fig. 8. Energy decay of $u(x,t)$ in the alternating case, computed in the time-range $\eta^2/\nu \leq t \leq L^2/\nu$. The last point on each curve corresponds to $t = L^2/\nu$. Dashed lines show the asymptotic result (45) valid for both fractal and spiral alternating pulse fields.

3.2. *Linear diffusive decay of non-alternating pulse fields: energy trapping*

3.2.1. *Homogeneous fractals*

The energy spectrum of homogeneous fractal non-alternating pulse fields is given by (21)–(23), and therefore

$$E(t) \sim \frac{(mN)^2}{L^2} + \frac{(mN)^2}{L} \int_{1/L}^{1/\eta} (kL)^{-D} \mathrm{e}^{-2\nu k^2 t}\, \mathrm{d}k \quad \text{for } \frac{\eta^2}{\nu} \ll t \ll \frac{L^2}{\nu}.$$

By noting that $E_\eta = \int_0^{1/\eta} E_0(k)\, \mathrm{d}k \sim ((mN)^2/L^2)(L/\eta)^{1-D}$ and by expanding the above integral (Appendix G) we are led to

$$\frac{E(t)}{E_\eta} \sim \left(\frac{\sqrt{\nu t}}{\eta}\right)^{-1+D} + \mathrm{O}\big((\eta/L)^{1-D}\big) \quad \text{for } \frac{\eta^2}{\nu} \ll t \ll L^2/\nu \tag{47}$$

in the limit where $\eta/L \to 0$. The term $\mathrm{O}((\eta/L)^{1-D})$ is negligible in front of $(\sqrt{\nu t}/\eta)^{-1+D}$ because $t \ll L^2/\nu$.

Again, the classical $t^{-1/2}$ result is recovered when $D = 0$. However, comparing (47) with (45), the space-filling property of fractals has exactly opposite effects on the decay of alternating and non-alternating pulse fields. The energy of homogeneous fractal non-alternating pulse fields decays slower for larger values of D. The more space-filling the fractal distribution of non-alternating pulses, the slower the structure decays. We call this effect "energy trapping" because the energy is trapped as a result of the space-filling property of the non-alternating pulse field. For larger Kolmogorov capacities D and therefore more space-filling fractals, non-alternating pulse fields are more autocorrelated (because $E_0(k) \sim k^{-D}$ in the range $1/L \ll k \ll 1/\eta$) and therefore decay more slowly; whereas

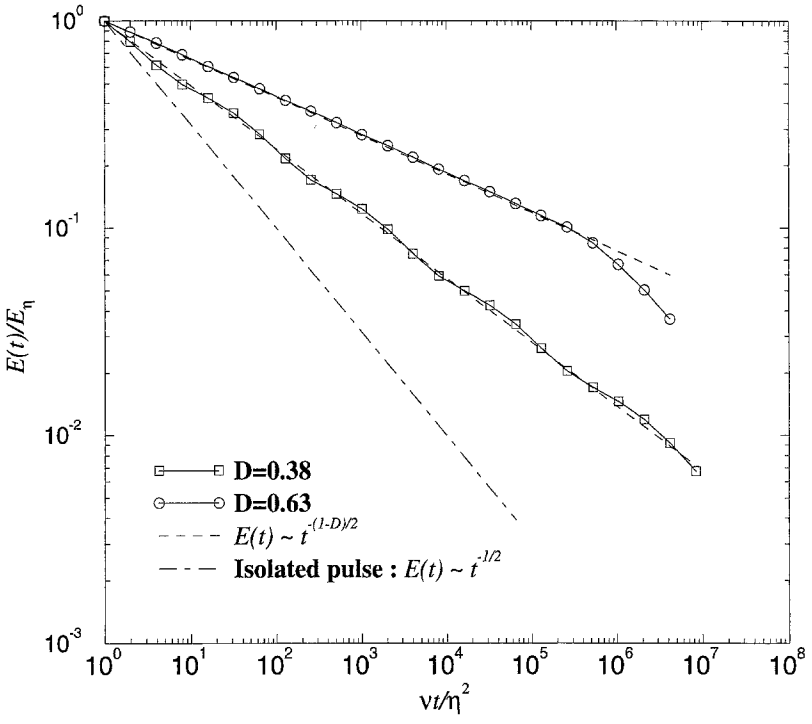

Fig. 9. Energy decay of $u(x, t)$ in the non-alternating case, for the Cantor set. Computation is performed in the time-range $\eta^2/\nu \leq t \leq L^2/\nu$. The last point on each curve corresponds to $t = L^2/\nu$. Dashed lines show the asymptotic result (47) valid for fractal non-alternating pulse fields only.

alternating pulse fields are less autocorrelated (because $E_0(k) \sim k^D$ in the range $1/L \ll k \ll 1/\eta$) and therefore decay faster. A low degree of autocorrelation reflects high irregularity in the field (for example a large number of high gradients) and, vice versa, a high degree of autocorrelation reflects high regularity in the field. The less regular the field, the faster it decays by diffusion, and this is why fractal non-alternating pulse fields with low Kolmogorov capacity D decay faster than fractal non-alternating pulse fields with high Kolmogorov capacity D.

The energy decay (47) is confirmed numerically by computing the energy of $u(x, t)$ from Eq. (46) (Fig. 9).

3.2.2. *Spirals*

The energy spectrum of spiral non-alternating pulse fields is different from that of homogeneous fractal non-alternating pulse fields and is given by (40)–(42). The calculation of the energy is performed using the same method as above. We have

$$E(t) = \int_0^{+\infty} E(k, t)\,\mathrm{d}k \simeq \frac{(Nm)^2}{L} x_N^{-1} + \frac{(Nm)^2}{L} x_N^{-1} \int_{x_N^{-1}}^{\eta^{-1}} k^{-1} \mathrm{e}^{-2\nu k^2 t}\,\mathrm{d}k$$

in the time-range $\eta^2/\nu \ll t \ll x_N^2/\nu$. Because $E_\eta = \int_0^{\eta^{-1}} E_0(k)\,\mathrm{d}k = ((Nm)^2/L)x_N^{-1}[1 + \ln(x_N/\eta)]$, it follows that

$$\frac{E(t)}{E_\eta} \sim \frac{1 + \int_{x_N^{-1}}^{\eta^{-1}} k^{-1} \mathrm{e}^{-2\nu k^2 t}\,\mathrm{d}k}{1 + \ln(x_N/\eta)}$$

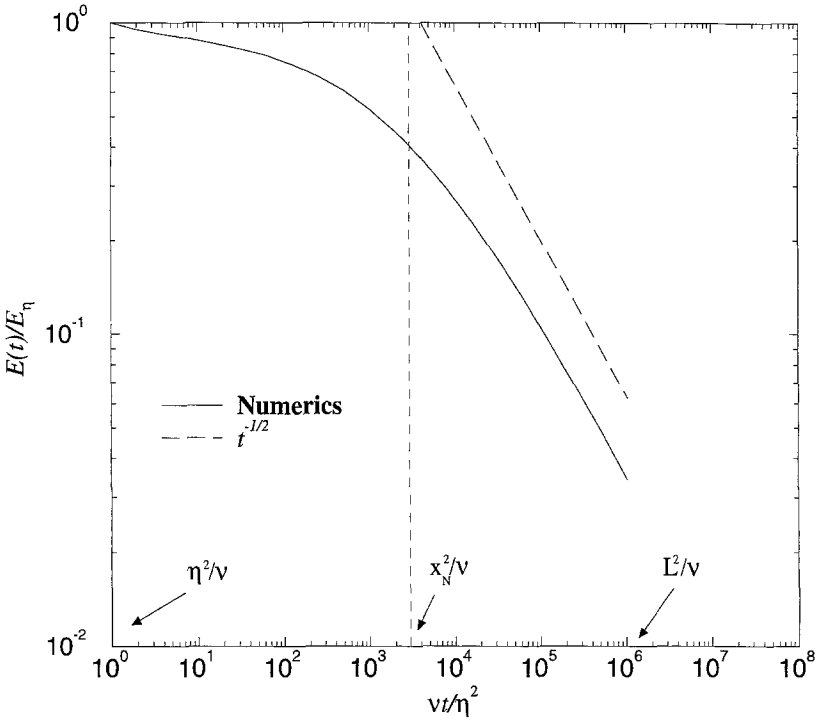

Fig. 10. Energy decay of $u(x,t)$ in the spiral case with non-alternated signs. The Kolmogorov capacity of this set of discontinuity points is $D = 0.7$.

in this time range. The integral $\int_{x_N^{-1}}^{\eta^{-1}} k^{-1} e^{-2\nu k^2 t}\, dk$ may be approximated by $\ln(x_N/\sqrt{\nu t})$ (see Appendix G), and therefore,

$$\frac{E(t)}{E_\eta} \sim \frac{\ln(x_N/\sqrt{\nu t})}{\ln(x_N/\eta)} + O\left(1/\ln\left(\frac{x_N}{\eta}\right)\right) \quad \text{for } \frac{\eta^2}{\nu} \ll t \ll \frac{x_N^2}{\nu}. \tag{48}$$

For times $t \gg x_N^2/\nu$,

$$E(t) \approx \int_0^{x_N^{-1}} E_0(k) e^{-2\nu k^2 t}\, dk \sim \frac{m^2 N^2}{L\sqrt{\nu t}}\left(\sqrt{\pi} + o(\exp(-2\nu t/x_N^2))\right). \tag{49}$$

In Fig. 10 we plot the results of a numerical computation of energy from Eq. (46) with $m_i = m$, confirming the laws (48) and (49).

Energy trapping is dramatically more effective by spiral rather than homogeneous fractal non-alternating pulse fields, but over a reduced time-range. The energy of a spiral non-alternating pulse field decays only logarithmically, and therefore at a dramatically slower rate than the energy of a homogeneous fractal non-alternating pulse field of any Kolmogorov capacity D. However, the energy of a spiral non-alternating pulse field decays logarithmically only over the reduced time-range $\eta^2/\nu \ll t \ll x_N^2/\nu$. Note, however, that this time-range increases as D increases, whereas the logarithmic decay of the energy as such remains unaffected. This is a reflection of the idiosyncratic way in which a spiral non-alternating pulse field becomes more autocorrelated as D increases. For times longer than x_N^2/ν, the time-dependence of the energy decay is given by (49) and is the same as that of one isolated pulse

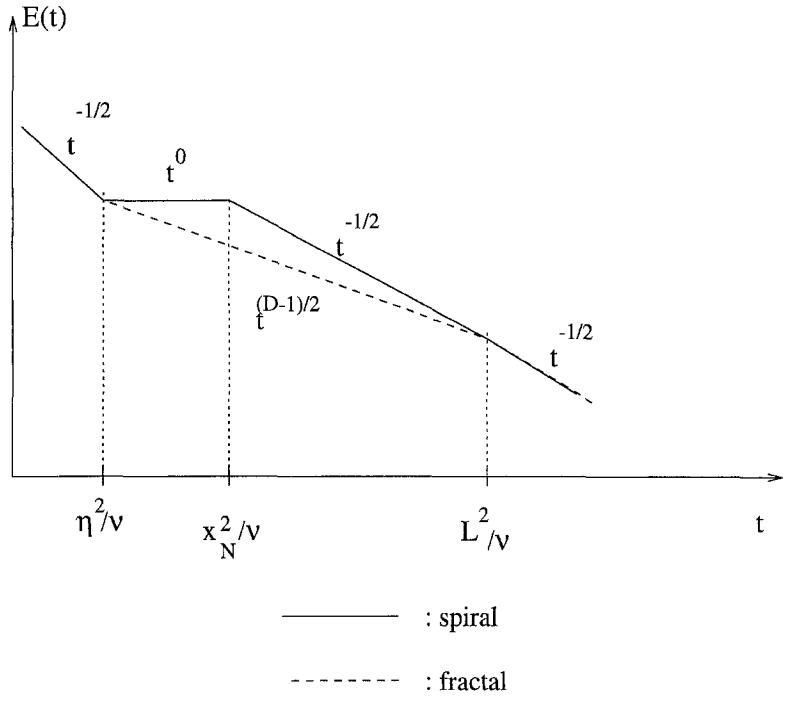

Fig. 11. Sketch of the energy decay of $u(x,t)$, for homogeneous fractals (dashed line) and for spirals (solid line), in the non-alternating case. In the spiral case the energy is trapped in the time range $\eta^2/\nu \ll t \ll x_N^2/\nu$, whereas in the homogeneous fractal case diffusion trapping is reflected in the slower scale-invariant energy decay from η^2/ν to L^2/ν.

with "mass" ($\int u\,\mathrm{d}x$) approximatively equal to the total mass of the structure (Nm). This corresponds to the fact that during the time range $\eta^2/\nu \ll t \ll x_N^2/\nu$ the merging of pulses located in the vicinity of the accumulation point have produced a "large" pulse containing almost all the mass of the initial structure. Fig. 11 shows a sketch of the energy decay in the spiral and fractal non-alternating cases.

Energy trapping is an effect of the non-alternating property that fractal and spiral fields can have, as the merging of neighbouring non-alternating pulses delay their energy decay. But spiral energy trapping is different from homogeneous fractal energy trapping.

3.3. Correlation length and diffusive length-scale

To achieve a more complete understanding of accelerated diffusion, Vassilicos [19] (see also [6]) calculated the time-dependence of the correlation length $\mathcal{L}(t)$ of fractal and spiral on–off fields. The integral

$$\mathcal{L}(t) = \int_0^\infty k^{-1} \frac{E(k,t)}{E(t)}\,\mathrm{d}k \tag{50}$$

is finite in the case of fractal and spiral on–off fields or alternating pulse fields. Vassilicos [19] defined the "diffusive length scale" $\delta(t)$ as

$$\delta(t) = \mathcal{L}(t) - \mathcal{L}(0), \tag{51}$$

which can be thought of as the scale over which the effects of diffusive attrition are appreciable [19]. In the non-alternating case the integral defining $\mathcal{L}(t)$ is low-wavenumber divergent at all times because $E_0(k) \sim (m^2/L)N^2 > 0$ for small Lk. To avoid this low-wavenumber divergence, we redefine $\mathcal{L}(t)$ by integrating the weighted scale $k^{-1}E(k,t)\,\mathrm{d}k/E(t)$ over the wavenumber range $[L^{-1}, +\infty[$ instead of $[0, +\infty[$, so that $\mathcal{L}(t)$ only contains information about the energy-containing scales below the overall length-scale of the structure. Moreover, by redefining

$$\mathcal{L}(t) = \lim_{l\to 0} \frac{\int_{L^{-1}}^{l^{-1}} k^{-1} E(k,t)\,\mathrm{d}k}{\int_{L^{-1}}^{l^{-1}} E(k,t)\,\mathrm{d}k},$$

we avoid an indefinite $\mathcal{L}(0)$, and in fact $\mathcal{L}(0) = 0$ for both homogeneous fractal and spiral pulse fields, in agreement with the fact that the thickness of delta functions is zero.

Let us now make use of the results for $E_0(k)$ and $E(t)$ obtained in this paper's previous sections. We are led to the following leading order results:

– *Alternating pulse fields, whether fractal or spiral:*

$$\delta(t) \sim \sqrt{\nu t} + \mathrm{O}\left(L\left(\frac{\sqrt{\nu t}}{L}\right)^{1+D}\right) \quad \text{for } \eta^2/\nu \ll t \ll L^2/\nu. \tag{52}$$

– *Non-alternating homogeneous fractal pulse fields:*

$$\delta(t) \sim \sqrt{\nu t} N_{\mathrm{boxes}}(\sqrt{\nu t}) + \mathrm{O}(\sqrt{\nu t}) \quad \text{for } \eta^2/\nu \ll t \ll L^2/\nu. \tag{53}$$

– *Non-alternating spiral pulse fields:*

$$\delta(t) \sim \frac{x_N}{\ln(x_N/\sqrt{\nu t})} + \mathrm{O}\left(\frac{\sqrt{\nu t}}{\ln(x_N/\sqrt{\nu t})}\right) \quad \text{for } \eta^2/\nu \ll t \ll x_N^2/\nu \tag{54}$$

and

$$\delta(t) \sim \sqrt{\nu t}\left(\ln\left(\frac{L^2}{2\nu t}\right) + \mathrm{O}(1)\right) \quad \text{for } x_N^2/\nu \ll t \ll L^2/\nu. \tag{55}$$

3.4. Phenomenology

Because the growth of the correlation length $\mathcal{L}(t)$ is caused by diffusion, we interpret the diffusion length-scale defined by (51) in the same way that it was interpreted by Vassilicos [19]: as a measure of the distance over which the effects of molecular diffusion are appreciable on the spatial structure of the field at time t. The diffusive length-scale of alternating pulse fields is not affected by the geometry of the structure, whereas the diffusive length-scale of non-alternating pulse fields is. This difference may be explained by noticing that two neighbouring pulses with same sign (and same strength) diffuse into a single pulse and that this process affects the diffusion length-scale, whereas two pulses with opposite sign (and same strength) never merge into a single pulse, so that the diffusive length-scale is only affected by the increase of the thickness of individual pulses, which is given by $\sqrt{\nu t}$.

Also of note, the diffusive length-scale of fractal and spiral non-alternating pulse fields is larger than $\sqrt{\nu t}$ in an intermediate range of times. This is in agreement with the fact that the presence of accumulation points enhances the merging of pulses, but this effect is very sensitive to the homogeneity of the structure. In the case of homogeneous fractal pulse fields, $\delta(t) \sim \sqrt{\nu t} N_{\mathrm{boxes}}(\sqrt{\nu t}) \sim (\nu t/L^2)^{(1-D)/2}$ in the time-range $\eta^2/\eta \ll t \ll L^2/\nu$, which means that during this time-range the diffusive length-scale $\delta(t)$ is proportional to the total length of the fractal covering by segments of size $\sqrt{\nu t}$. In the case of spiral pulse fields, $\delta(t) \sim x_N/\ln/\sqrt{\nu t})$ for as long as $\eta \ll \sqrt{\nu t} \ll x_N$. This

is due to the fact that the merging of pulses located near the single accumulation point of the spiral structure have produced a large pulse with a scale much larger than the scale of pulses located far from the accumulation point.

We now use the expressions obtained for the diffusive length-scale $\delta(t)$ in a short-cut phenomenological argument which leads to and sheds some additional light onto the laws of energy decay of Sections 3.1 and 3.2. The integral $\int u(x,t)\,\mathrm{d}x$ is conserved in time by the linear diffusion equation (1). By virtue of our interpretation of $\delta(t)$, for both alternating and non-alternating pulse fields we may estimate that

$$\int u(x,t)\,\mathrm{d}x \sim U(t)\delta(t),$$

where $U(t)$ is a positive characteristic value of the pulse field $u(x,t)$, for example a typical maximum absolute value of pulses. For alternating pulse fields, $\int u(x,t)\,\mathrm{d}x \sim m$ and for non-alternating pulse fields, $\int u(x,t)\,\mathrm{d}x \sim Nm$. Hence,

$$U(t) \sim \frac{m}{\delta(t)}$$

for alternating pulse fields, and

$$U(t) \sim \frac{Nm}{\delta(t)}$$

for non-alternating pulse fields.

The energy $E(t)$ is given by $(1/L)\int u^2(x,t)\,\mathrm{d}x$ and we estimate that

$$\int u^2(x,t)\,\mathrm{d}x \sim U^2(t)\sqrt{\nu t}N_{\mathrm{boxes}}(\sqrt{\nu t})$$

for alternating pulse fields, whereas

$$\int u^2(x,t)\,\mathrm{d}x \sim U^2(t)\delta(t)$$

for non-alternating pulse fields. It follows that

$$E(t) \sim \frac{m^2}{L\delta^2(t)}\sqrt{\nu t}N_{\mathrm{boxes}}(\sqrt{\nu t}) \tag{56}$$

for alternating pulse fields and that

$$E(t) \sim \frac{N^2m^2}{L\delta(t)} \tag{57}$$

for non-alternating pulse fields. By inserting the expressions for $\delta(t)$ obtained in Section 3.3 into (56) and (57) we recover the laws of energy decay (45), (47)–(49).

4. Anomalous collision rate in the Burgers equation

We now show how the anomalous diffusive properties investigated above have remarkable effects on the diffusion/convection problem. We study the decay of alternating and non-alternating one-dimensional fractal or spiral velocity fields $u_0(x)$ (Eq. (3) with $m_i = (-1)^{i+1}m$ or $m_i = m$, and Fig. 1), when submitted to convective and diffusive transport according to Eq. (2). If $u_0(x)$ is an isolated pulse with integral $\int u_0(x)\,\mathrm{d}x = m$ it is interesting to consider the ratio m/ν, which may be thought of as the Reynolds number of the pulse.

When $m/\nu \gg 1$, convective transport dominates over viscous diffusion, and instantly leads to the formation of a shock moving on the x-axis [2,12,16,17]. If the initial pulse has a length l the shock appears when $t \gg l^2/m$. After shock formation the energy of the isolated one-signed pulse decays as

$$E(t) = \frac{2^{3/2}}{3L}\frac{m^{3/2}}{t^{1/2}}. \tag{58}$$

When there are many shocks, they are likely to collide, and these collisions are known to delay the energy decay [9,12,17]. In Section 4.1 we write the solution of the Burgers equation corresponding to the field u_0 defined in (3), then we analyse the effect of collisions on the evolution of $u(x,t)$.

4.1. Solution of the Burgers equation

The solution of the Burgers equation for an initial field equal to one delta function has been given by Benton and Platzman [2], and can be easily generalized to a sum of delta functions u_0 (Eq. (3)). The Hopf–Cole transformed field of $u_0(x)$ is defined by

$$\theta_0(x) = \mathrm{e}^{-(1/2\nu)\psi_0(x)},$$

where ψ_0 is the integral of u_0. If we assume that $x_1 < x_2 < \cdots < x_N$, it follows from (3) that

$$\psi_0(x) = \sum_{i=1}^{j(x)} m_i \quad \text{for } x > x_1,$$

where the index $j(x)$ is defined by $x_{j(x)} < x < x_{j(x)+1}$, and $\psi_0(x) = 0$ for $x < x_1$. Hence,

$$\theta_0(x) = \mathrm{e}^{-(1/2\nu)\sum_{i=1}^{j(x)} m_i} \quad \text{for } x > x_1,$$

$\theta_0(x) = 1$ for $x < x_1$, and θ_0 is a step function which can be written as

$$\theta_0(x) = 1 + \sum_{i=1}^{N} (\mathrm{e}^{-(1/2\nu)M_i} - \mathrm{e}^{-(1/2\nu)M_{i-1}}) H(x - x_i),$$

where $M_i = \sum_{j=1}^{i} m_j$ and $M_0 = 0$. H denotes the Heaviside function. Because θ_0 is submitted to a linear diffusive process, the evolution of each Heaviside function is given by an error-function, so that $\theta(x,t)$ reads

$$\theta(x,t) = 1 + \sum_{i=1}^{N} (\mathrm{e}^{-(1/2\nu)M_i} - \mathrm{e}^{-(1/2\nu)M_{i-1}}) \frac{1}{2}\left[\mathrm{erf}\left(\frac{x - x_i}{2\sqrt{\nu t}}\right) + 1\right] \tag{59}$$

for all times t, positions x, viscosity ν, discontinuity points $(x_i)_{i=1,\ldots,N}$ and "masses" M_i. The velocity field is then obtained from Eq. (8). The fact that gradients turn into universal shocks if the Reynolds number is sufficiently large makes it convenient to analyse the Burgers equation in the limit $\nu \ll m$ in terms of the creation, displacement and collisions of shocks [12,17]. However, in this paper, we use $\theta(x,t)$ as given in (59) to predict the time when shocks interact, by noticing that collision events in $u(x,t)$ correspond to diffusion events in $\theta(x,t)$.

4.2. Energy decay for large Reynolds number

4.2.1. Alternating pulse field

When N is even and the first pulse is positive, every pulse in $u(x,t)$ collides with its neighbour, and because every two pulses have the same strength, they eventually form a single shock which does not move on the x-axis.

Thus, the total energy of the signal decays like t^{-2} [17] after the first collision. When N is even and the first pulse is negative, the first shock and the last shock move freely on the x-axis, and the energy decays like $t^{-1/2}$. When N is odd, the first or last pulse moves freely on the x-axis, and its energy therefore decays like $t^{-1/2}$. In both cases N even and N odd, the law of energy decay is independent of the Kolmogorov capacity of the points (x_i).

4.2.2. Non-alternating pulse field

We see from Eq. (59) that the gradient field $\partial\theta/\partial x$ is a sum of initially delta-functions gradually smoothed into gaussian functions (see Fig. 12). Each gaussian in $\partial\theta/\partial x$ corresponds to one single shock in u. It two consecutive shocks of index i and $i+1$ do not interact, $\partial\theta/\partial x$ displays a plateau between the gaussian centred around x_i and the one centred around x_{i+1} (Fig. 12). Interaction between the two shocks corresponds to the gaussian centred around x_i being no more negligible in the vicinity of x_{i+1} in comparison to the gaussian centred around x_{i+1}, and a collision between the two shocks corresponds to the merging of the two gaussians. From this observation we extract two important smoothing times for $\partial\theta/\partial x$. The first one is the time when the two closest pulses in $\partial\theta/\partial x$ are smoothed by diffusion. The distance between these pulses is

$$\eta = \min_{i=1,N-1}(x_{i+1} - x_i) = x_{\gamma+1} - x_\gamma.$$

We define t_η as the time when the gaussian centred around x_γ is of the order of the gaussian centred around $x_{\gamma+1}$ at $x = x_{\gamma+1}$, which means that the plateau between these two pulses has vanished. By making use of (59) we get

$$(\mathrm{e}^{-(1/2\nu)M_\gamma} - \mathrm{e}^{-(1/2\nu)M_{\gamma-1}}) \exp\left(-\frac{\eta^2}{4\nu t_\eta}\right) \sim \mathrm{e}^{-(1/2\nu)M_{\gamma+1}} - \mathrm{e}^{-(1/2\nu)M_\gamma},$$

and by noticing that $M_i = i\,m$ we get

$$t_\eta \sim \frac{\eta^2}{2m}. \tag{60}$$

In terms of shocks in u, t_η is the time when the interaction between the two closest shocks starts, and result (60) is in agreement with the fact that an isolated positive shock moves like $(2mt)^{1/2}$ [16,17]. Another important time scale is the time when all the pulses in $\partial\theta/\partial x$ are smoothed out by diffusion, say t_L. From (59) we get

$$t_L \sim \frac{1}{2m}\frac{(x_N - x_1)^2}{N-1} \simeq \frac{1}{2m}\frac{L^2}{N}. \tag{61}$$

In terms of shocks in u, t_L can be thought of as the time when all the collisions have been completed. Note that if the structure has a well-defined Kolmogorov capacity D we have $N \sim (\eta/L)^{-D}$ and

$$t_L \sim \frac{\eta^2}{2m}\left(\frac{\eta}{L}\right)^{D-2}. \tag{62}$$

In the following we calculate the energy decay of $u(x,t)$ in the time range $t_\eta < t < t_L$ for non-alternating homogeneous fractal and spiral pulse fields.

4.2.2.1. Non-alternating homogeneous fractal pulse fields. The case of pulses on a Cantor set has been treated by Gurbatov and Crighton [9] who observe that the delay of energy decay increases with D. Here we show that the law of energy decay found by these authors can also be obtained for any homogenous fractal non-alternating pulse field under the assumption that the energy decays in a scale-invariant manner between t_η and t_L.

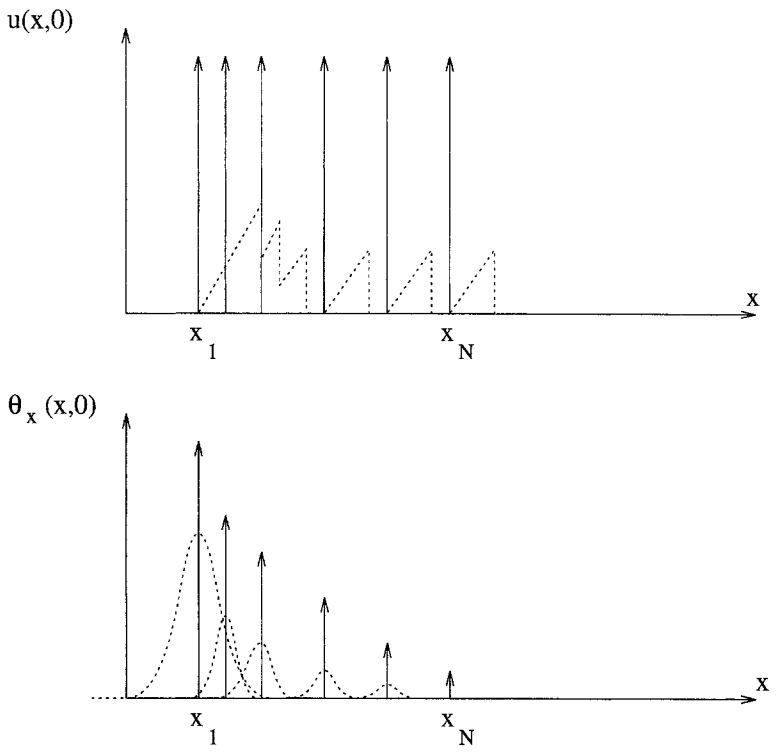

Fig. 12. Sketch of the non-alternating pulse field $u(x,t)$, and of the derivative of its Hopf–cole transformed field $\theta_x(x,t) = \partial\theta/\partial x$. Solid lines show both fields at $t = 0$. θ_x is a sum of delta-functions located at $x_1, \ldots, x_N$. The strength of the pulses of θ_x decays exponentially with the index of the position. As θ_x undergoes a diffusive process, its delta-functions turn into gaussian pulses (dashed line, lower graph) which correspond to shocks in u (dashed line, upper graph). When two gaussian pulses in θ_x overlap the two corresponding shocks interact in u, and the merging of two consecutive gaussians in θ_x corresponds to a collision between two consecutive shocks in u. Due to the space-filling feature of the (x_i), the smoothing of θ_x is very fast, and induces an anomalous collision rate in $u(x,t)$, and therefore a huge delay in the energy of $u(x,t)$.

Before the first collision ($t < t_\eta$) the energy of the signal evolves as

$$E(t) = N \times \frac{2^{3/2}}{3L}\frac{m^{3/2}}{t^{1/2}}, \quad t < t_\eta,$$

since the signal is made of N isolated (i.e. non-interacting) shocks. For $t > t_L$ the velocity field is made of a single shock the integral of which is $N\,m$. The energy of the signal is then

$$E(t) = \frac{2^{3/2}}{3L}\frac{(Nm)^{3/2}}{t^{1/2}}, \quad t > t_L.$$

At this stage let us conjecture that for non-alternating homogeneous fractal fields of pulses of equal strength m the energy decays in a scale-invariant manner between t_η and t_L:

$$E(t) \simeq E(t_\eta)\left(\frac{t}{t_\eta}\right)^{-\beta}, \quad t_\eta < t < t_L.$$

By making use of Eqs. (60) and (62), and by noticing that

$$E(t_\eta) \simeq N \times \frac{2^{3/2}}{3L}\frac{m^{3/2}}{t_\eta^{1/2}} \quad \text{and} \quad E(t_L) \simeq \frac{2^{3/2}}{3L}\frac{(Nm)^{3/2}}{t_L^{1/2}},$$

we obtain the exponent β, and therefore the law of energy decay

$$E(t) \sim E(t_\eta)\left(\frac{2mt}{\eta^2}\right)^{-(D-1)/(D-2)}, \quad t_\eta < t < t_L. \tag{63}$$

This is the law obtained by Gurbatov and Crighton [9] who investigated the decay of a Cantor set of triangular pulses. Note that this law only requires the assumptions of scale-invariant geometry (5) and of scale-invariant energy decay. This law is not expected to hold for inhomogeneous fractal pulse fields, because scale-invariant decay is not expected to hold there.

4.2.2.2. Non-alternating spiral pulse fields. In the case of non-alternating pulse fields we again observe significant differences between homogeneous fractals and spirals, due the strong inhomogeneity of spirals. Here also, the scale x_N plays an important role, as shown in Fig. 13, where we have plotted the curve $Y = \psi_0(X)$, together with the parabola

$$P_A : Y = A - (X - x)^2/(2t),$$

which enables to determine the velocity potential $\psi(x, t)$ for $t > 0$ (see for example [7,12,17]). Briefly, for all x and t, $\psi(x, t)$ is given by the maximal A such that the parabola P_A lies below the curve $Y = \psi_0(X)$. The point (X, Y) corresponding to this maximum is interpreted as the first contact point of the curve $Y = \psi_0(X)$ and the parabola.

The spiral investigated in this paper is given by $x_i = Li^{-\alpha}$, and therefore the shape of ψ_0 is

$$\psi_0(X) = \int_0^X u_0(x)\,\mathrm{d}x \sim m(N - p) \sim m\left(N - \left(\frac{X}{L}\right)^{-1/\alpha}\right), \tag{64}$$

where $N - p$ is the number of discontinuity points lying between 0 and X. Clearly, $\psi_0(X)$ is zero for $X < x_N$ (Fig. 13). For a fixed position x between x_N and L, one can notice that if t is small enough, the first contact point (X, Y) is close to $(x, \psi_0(x))$, whereas for t larger than some critical time $\tau(x)$, P_A will intersect the curve

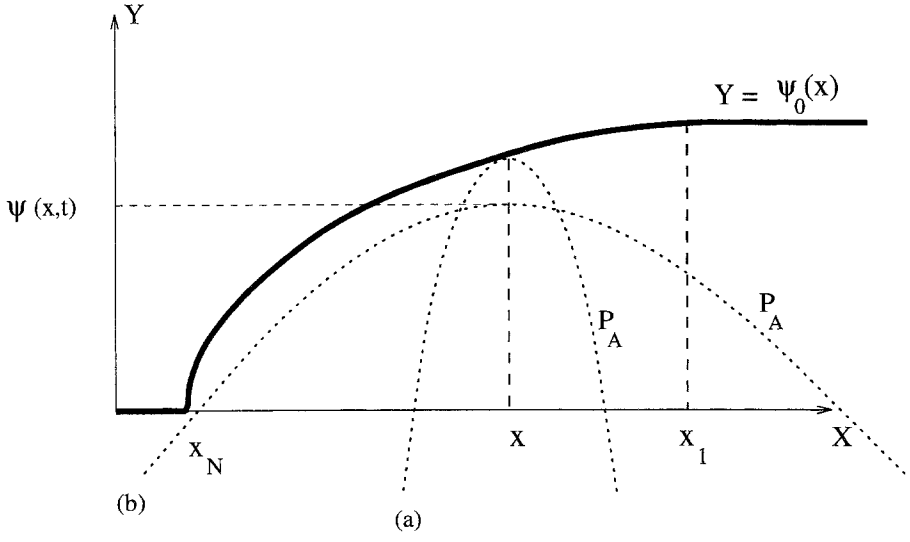

Fig. 13. Sketch of the initial velocity potential ψ_0 together with the parabola P_A: (a) $t < \tau(x)$; (b) $t > \tau(x)$.

$Y = \psi_0(X)$ at $X = x_N$, and this point will remain the first contact point for all $t > \tau(x)$. It is at this stage that the inhomogeneity of the spiral manifests itself, in a way determined by the scale x_N. By writing that $x_N \in P_A$ we get

$$\psi(x,t) = \frac{(x_N - x)^2}{2t} \quad \text{for } t > \tau(x),$$

so that the velocity potential for $t > \tau(x)$ does not depend on ψ_0, and therefore does not feel the spiral geometry of the structure. The critical time $\tau(x)$ is such that $\psi_0(x, \tau(x)) \simeq \psi_0(x)$, and therefore reads

$$\tau(x) \simeq \frac{(x_N - x)^2}{2mN(1 - (x/x_N)^{-1/\alpha})}, \tag{65}$$

which can be shown to be the time required for the smoothing of the pulses of $\partial\theta/\partial x$ located between x_N and x. $\tau(x)$ is therefore the time when the first shock reaches the position x, so that the spiral structure of the field $u(x,t)$ is no more visible between x_N and x. It is convenient to inverse eq. (65) to obtain the critical position $x_c(t)$ where P_A intersects the curve $Y = \psi_0(X)$ at $X = x_N$, for a given time t. If $(x_c(t)/x_N)^{-1/\alpha} \ll 1$, which is verified if $x_c(t) \gg x_N$, we have

$$x_c(t) \simeq x_N + \sqrt{2Nmt}.$$

Therefore the integral of $\psi(x,t)$ over the whole structure can be written

$$\langle\psi\rangle = \frac{1}{L}\int_0^L \psi(x,t)\,\mathrm{d}x \simeq \frac{1}{L}\int_{xN}^{x_N+\sqrt{2Nmt}} \frac{(x_N - x)^2}{2t}\,\mathrm{d}x + \frac{1}{L}\int_{x_N+\sqrt{2Nmt}}^{L} \psi_0(x)\,\mathrm{d}x,$$

where the LHS integral is performed over the points x for which the parabola has already reached $x_N (x < x_c(t))$, and the RHS integral is performed over the points x for which the parabola has not yet reached $x_N (x > x_c(t))$. By integrating Eq. (2) we get

$$E(t) = -\frac{\mathrm{d}\langle\psi\rangle}{\mathrm{d}t} \simeq \frac{1}{L}\psi_0(x_N + \sqrt{2Nmt})\frac{\sqrt{Nm}}{\sqrt{2t}} - \frac{1}{3L}\frac{(Nm)^{3/2}}{\sqrt{2t}}.$$

Finally, for $\sqrt{2Nmt} \gg x_N$ we can expand $\psi_0(x_N + \sqrt{2Nmt})$ by making use of Eq. (64), and we get

$$E(t) \simeq \frac{2^{1/2}}{3L}\frac{(Nm)^{3/2}}{t^{1/2}} - \mathrm{O}\left(\left(\frac{\sqrt{2Nmt}}{x_N}\right)^{-1/\alpha-1}\right), \quad x_N^2/Nm \ll t \ll t_L \sim L^2/Nm. \tag{66}$$

Hence, the energy decay for $t \gg x_N^2/Nm$ is at leading order similar to the decay of an isolated pulse ($E(t) \sim t^{-1/2}$). This is surprising in that collisions still occur in the time range $x_N^2/Nm \ll t \ll L^2/Nm$, but these collisions seem to have very little effect on the energy decay.

Fig. 14 shows the energy decay for a spiral with $D = 0.7$, computed from the analytical solution of Eq. (2) in the limit $\nu \to 0$ [12]. Note that the energy displays a plateau for $\eta^2/m \ll t \ll x_N^2/Nm$, in agreement with the fact that the collision rate is huge in this time range. Also of note, the waves visible on this curve for $t \gg x_N^2/Nm$ correspond to collisions which have almost no effect on the energy decay.

4.2.3. Phenomenology: smoothing of θ and collisions in u

The laws of energy decay calculated in Sections 4.2.1 and 4.2.2 can be understood in terms of the collision rate between shocks [17]. Here we draw a parallel between this collision rate and the speed of the smoothing of $\partial\theta/\partial x$.

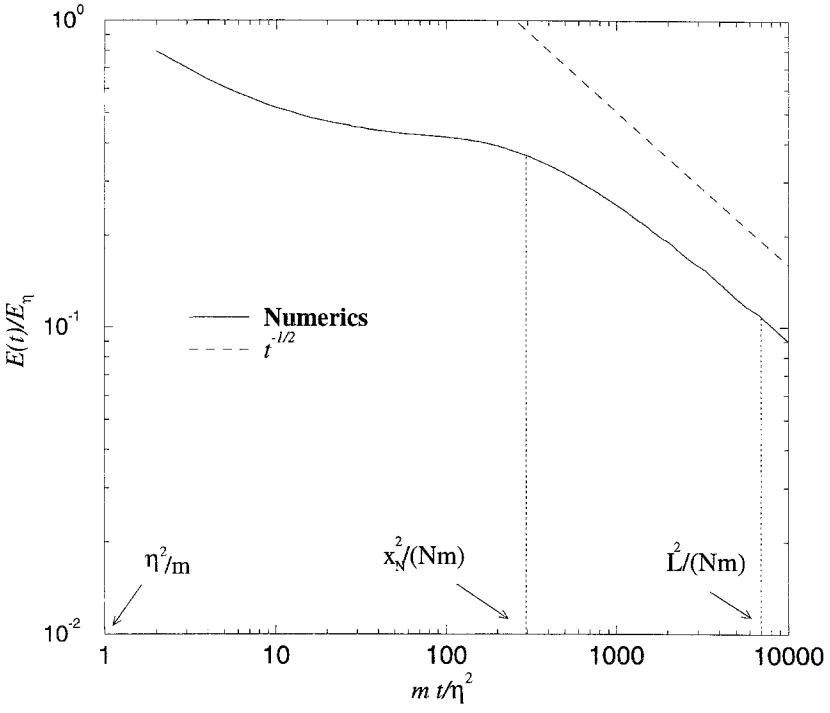

Fig. 14. Energy decay (Burgers equation) of non-alternating pulses distributed in a spiral manner, for $\nu \ll m$. Like for the linear diffusion equation, some energy trapping is observed on a time range fixed by the inhomogeneity scale x_N. $L^2/(N_m)$ is the time of the last collision.

4.2.3.1. Alternating pulse field. Because $m_i = m(-1)^{i+1}$ we have $M_i = 0$ if i is even and $M_i = m$ if i is odd, and from Eq. (59) we conclude that $\partial\theta_0/\partial x$ is an alternating pulse field, the strength of the pulses being constant in absolute value (and equal to $\exp(-m/2\nu)$). The diffusive length-scale $\delta_\theta(t)$ of $\partial\theta/\partial x$ can be thought of as the characteristic scale of the gradients of $\partial\theta/\partial x$, so that the growth of $\delta_\theta(t)$ corresponds to the smoothing of these gradients, and therefore to the disappearance of the shocks in $u(x,t)$. From Section 3 we know that $\delta_\theta(t)$ grows independently of D. Hence, the collision rate between the shocks of u is independent of D. This is in agreement with the fact that the energy decay has been found to be independent of D in this case (Section 4.2.1).

4.2.3.2. Non-alternating homogeneous fractal pulse field. In this case gaussian pulses in $\partial\theta/\partial x$ (Fig. 12) will merge, leading to a single gaussian pulse, and therefore to a single shock in u. The time-range over which all the collisions occur can be approximated by

$$t_\eta < t < t_L,$$

and the mean collision rate in this time range is therefore

$$\text{mean collision rate} = \frac{N-1}{t_L - t_\eta} \simeq \frac{2m}{\eta^2}\left(\frac{\eta}{L}\right)^{2(1-D)}.$$

For $D = 0$ the collision rate is $2m/L^2$. It corresponds to a collision occurring between two pulses separated by a distance L. As $D \to 1$ the collision rate tends to $2m/\eta^2 = 1/t_\eta$ which is much larger and corresponds to one collision every "small" convective time. The space-filling properties of the structure are therefore responsible for an

"anomalous collision rate" between shocks, and therefore to a significant delay of the energy decay, in agreement with the law (63).

4.2.3.3. Non-alternating spiral pulse field. A phenomenology similar to the one of the linear diffusion equation can be applied here. Indeed, for $\eta^2/m \ll t \ll x_N^2/Nm$ collisions occur very often in the vicinity of the accumulation point. This large collision rate is responsible for a significant delay of the energy decay in this time range, and produces a big shock containing an important fraction of the "mass" ($\int u\,\mathrm{d}x$) and of the energy of the whole structure. For $t \gg x_N^2/Nm$ the mass of this shock is such that new collisions have no more effect on it, and this shock decays like an isolated shock.

4.3. Energy decay for low Reynolds number

When $m \ll \nu$ diffusive effects are expected to overwhelm convective effects. Here we apply results of Section 3, together with the simple phenomenology developed in Section 3.4, to show how the space-filling properties of the signal can turn the linear decay into a nonlinear decay.

4.3.1. Homogeneous fractals

As the field diffuses, $u(x,t)$ is characterized by pulses with thickness $\sqrt{\nu t}$ and typical velocity $U(t)$, and their individual Reynolds number can be defined as

$$Re(t) = \frac{U(t)\sqrt{\nu t}}{\nu}.$$

Note that in the non-fractal case $U(t)$ decays like $t^{-1/2}$, so that $Re(t)$ remains unchanged. We estimate $U(t)$ by applying conservation of $\int u(x,t)\,\mathrm{d}x$ (Section 3.4). For short times we have $Re(t) \ll 1$, so that we can make use of the expressions for $\delta(t)$ obtained in Section 3.3 (diffusion equation). This leads to

$$Re(t) \sim \frac{m}{\nu} \ll 1$$

for alternating pulse fields, and

$$Re(t) \sim \frac{Nm}{\nu}\left(\frac{\sqrt{\nu t}}{L}\right)^D$$

for non-alternating pulse fields. As a result, the Reynolds number of individual pulses remains small for alternating pulse fields, but increases for non-alternating pulse fields, so that the linear decay can turn into a strongly nonlinear decay. Note that for $t = \eta^2/\nu$ we recover $Re \sim m/\nu$ since $N \sim (\eta/L)^{-D}$. This increase of the individual Reynolds number, which is a consequence of the scale-invariance of the structure, has been used by Gurbatov and Crighton [9] to justify the use of the inviscid hypothesis for pulses displayed on a Cantor set. Note that it requires $Nm/\nu \gg 1$. The critical time t_c when the transition between the linear and the nonlinear decay occurs corresponds to $Re \sim 1$ and reads

$$t_c = \frac{L^2}{\nu}\left(\frac{Nm}{\nu}\right)^{-2/D}.$$

Fig. 15 shows the energy decay corresponding to a Cantor set of pulses, calculated from the analytical solution (59) with $m/\nu = 1$ and $N = 1024$. It confirms the occurrence of a transition at $t = t_c$.

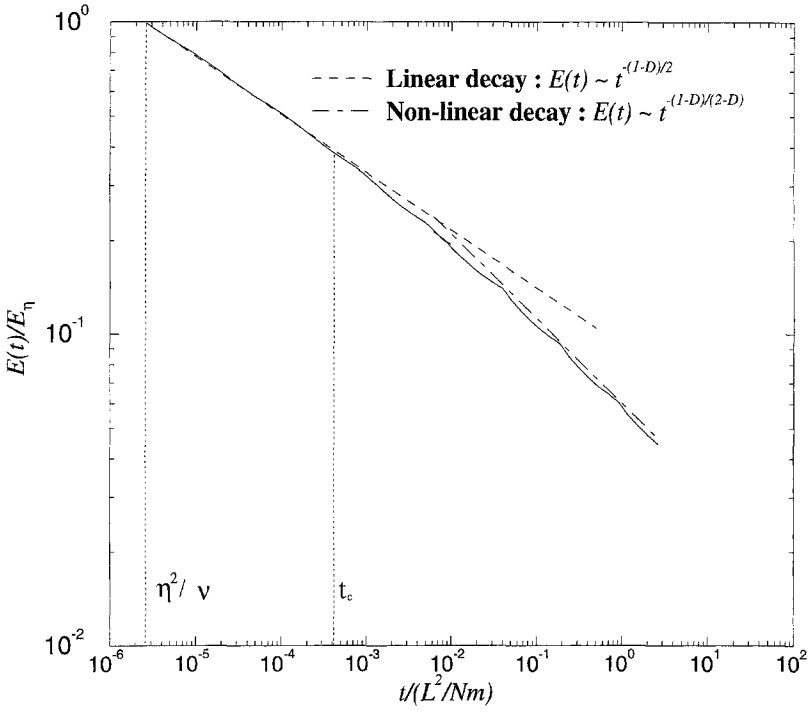

Fig. 15. Energy decay (Burgers equation) of non-alternating pulses distributed on a Cantor set of points, for $\nu > m$, calculated from the exact analytical solution of the Burgers equation (Eqs. (59) and (8)). Linear decay is observed for short times, then a transition occurs after the time t_c predicted by the theory. The analytical solution quits the linear law at $t \simeq t_c$, then blows-up after a decade, due to loss numerical accuracy. The run is continued with an inviscid solver for longer times.

4.3.2. Spirals

The case of spiral alternating pulse-fields is similar to the case of fractal alternating pulse-fields, as a consequence of their similar spectral properties. In the spiral non-alternating case pulses will start diffusing, as $\nu \gg m$. This merging will produce a strong pulse in the vicinity of x_N, with typical velocity $U(t)$ and thickness $\delta(t)$ which are much larger than those of other pulses (see Section 3.3). Accordingly, the individual Reynolds number of this pulse is

$$Re(t) = \frac{U(t)\delta(t)}{\nu}$$

for early times, and momentum conservation implies $U(t)\delta(t) \sim Nm$, so that we get

$$Re \sim \frac{Nm}{\nu}.$$

Hence, provided $Nm/\nu \gg 1$, the Reynolds number of this pulse will be large for $t \gg \eta^2/\nu$, and a nonlinear regime corresponding to the decay of an isolated shock with integral of order Nm will start.

5. Conclusion

We have analysed spectral, diffusive and convective properties of one-dimensional fractal and spiral pulse fields with alternating signs (lower graph of Fig. 1) and non-alternating signs (upper graph of Fig. 1). The integral of the alternating pulse field is an on–off function the spectrum and diffusive properties of which have

been investigated by Vassilicos and Hunt [20] and Vassilicos [19]. Such an on–off function may be obtained by performing a one-dimensional cut through a two-dimensional scalar field characterized by sharp interfaces with well-defined Kolmogorov capacity [20]. From a similar viewpoint, the non-alternating pulse field may correspond to a one-dimensional cut through a two-dimensional scalar field uniformly distributed along a fractal or spiral line.

The energy spectrum of the alternating pulse field scales like k^D for $L^{-1} \ll k \ll \eta^{-1}$ [20], for both fractal and spiral distributions of pulses. The energy spectrum of the non-alternating pulse field is found to scale like k^{-D} for $L^{-1} \ll k \ll \eta^{-1}$ in the homogeneous fractal case, and like k^{-1} for $x_N^{-1} \sim \eta^{-1}(\eta/L)^D \ll k \ll \eta^{-1}$ in the spiral case. In all cases the spectrum is flat over other wavenumber ranges. We therefore observe that the space-filling properties of the pulse field make it more regular (more autocorrelated) in the non-alternating case, whereas they make it more singular (less autocorrelated) in the alternating case. Moreover, the energy spectrum is very sensitive to the homogeneity of the structure in the non-alternating case, leading to differences between homogeneous fractals and spirals, whereas homogeneity does not matter in the alternating case. The scale x_N is characteristic of the inhomogeneity of the spiral set.

We have analysed the diffusive properties of these structures and observe that space-filling properties accelerate the energy decay of alternating pulse fields, in agreement with previous works by Vassilicos [19] and Flohr and Vassilicos [6]. However, space-filling properties are observed to *delay* the energy decay of non-alternating pulse fields, in such a way that energy is "trapped" during a time range fixed by the characteristic scales of the structure. The energy of both fractal and spiral distributions of alternating pulses decays in a scale-invariant manner between the time scales η^2/ν and L^2/ν, the power-law of this decay being entirely determined by the Kolmogorov capacity D. In contrast, the energy decay of non-alternating pulse fields is sensitive to the inhomogeneity of the structure. Indeed, the energy of spiral non-alternating pulse fields is almost constant (decays only logarithmically) in the time range $\eta^2/\nu \ll t \ll x_N^2/\nu$, then decays like $t^{-1/2}$ for longer times. This is a direct consequence of the inhomogeneity of the structure, as pulse merging is important in the vicinity of the isolated accumulation point and tends to form a huge pulse containing an important fraction of the "mass" ($\int u \, dx$) and of the energy of the spiral structure. The emergence of this large pulse therefore breaks the scale-invariance of the structure. This energy trapping is different from the one observed in homogeneous fractal non-alternating pulse fields, where the decay is slowed-down in a scale-invariant way over the whole range $\eta^2/\nu \ll t \ll L^2/\nu$.

The evolution of the diffusive length-scale brings in useful information about anomalous diffusion. The diffusive length-scale of alternating pulse fields is not sensitive to the space-filling properties of the structure and scales as $\sqrt{\nu t}$, whereas the diffusive length-scale of non-alternating pulse fields is significantly larger than $\sqrt{\nu t}$. This difference can be explained by noticing that pulse merging is a strongly correlating mechanism which is enhanced by the space-filling properties of the structure in the non-alternating case, whereas in the alternating case the correlation length-scale is mainly affected by the growth of individual pulses.

The diffusive length-scale is very sensitive to the inhomogeneity of the structure in the non-alternating case. Indeed, for $\eta^2/\nu \ll t \ll L^2/\nu$ we have $\delta(t) \sim \sqrt{\nu t} N_{\text{boxes}}(\sqrt{\nu t})$ for homogeneous fractal pulse fields, as already observed for fractal or spiral on–off functions [19], whereas for spiral pulse fields $\delta(t)$ growths only logarithmically (and $\delta(t) \gg \sqrt{\nu t}$) for $\eta^2/\nu \ll t \ll x_N^2/\nu$, then growths like $\sqrt{\nu t}$. These differences are in agreement with the fact that the structure is smoothed out in the same way everywhere on the homogeneous fractal, whereas pulse merging on spirals quickly produces a large pulse in the vicinity of the accumulation point, the characteristic scale of which is much larger than the scale of isolated pulses.

When submitted to a diffusive/convective process (Burgers equation) non-alternating pulse fields are observed to have interesting properties linked to their geometry. In contrast, in the inviscid limit, the decay of alternating pulse fields is not sensitive to the Kolmogorov capacity of the structure. However, as already shown for the Cantor set by Gurbatov and Crighton [9], the energy decay of non-alternating pulse fields in the inviscid limit strongly

depends on D. We notice that the law of energy decay of these authors can be established for any homogeneous fractal pulse field, assuming that the energy decay of such fields is scale-invariant. In contrast, the energy decay of spiral non-alternating pulse fields is not scale-invariant from the time of the first collision (η^2/m) to the time of the last collision (L^2/Nm), as it is roughly constant from η^2/m to x_N^2/Nm, then decays like for an isolated shock for longer times. The phenomenology involved in this process is very similar to that of the diffusion problem. Indeed, shock collisions in spirals occur very often in the vicinity of the accumulation point, whereas they occur with the same probability "everywhere" in a homogeneous fractal. In both cases, the huge delay of energy decay is a consequence of the large collision rate between shocks and is due to the space-filling feature of the structure. This "anomalous collision rate" is to be linked with the fact that the gradients of the Hopf–Cole transformed field undergo an accelarated diffusive smoothing.

We have investigated the Burgers equation with large viscosity ($\nu \gg m$) and observe that for non-alternating pulse fields the space-filling geometry can turn the linear decay into a nonlinear decay, as already noted by Gurbatov and Crighton [9]. Indeed, the merging of pulses, together with the scale-invariant feature of the structure, is responsible for a transition from the law of energy decay (47) (Section 3) to the law (63) (Section 4).

Finally, we stress that spectral, diffusive and convective properties of spiral non-alternating pulse fields are characterized by three scales, namely η, x_N, and L, whereas the spectra and dynamics of spiral alternating pulse fields (and spiral on–off fields) are not sensitive to the inhomogeneity length-scale x_N and are similar to the spectra and dynamics of homogeneous fractals.

Acknowledgements

We are grateful for financial support from the Royal Society, the EPSRC and the EEC's TMR programme.

Appendix A. Low-wavenumber energy spectrum in the alternating case

The Fourier transform of $u_0(x)$ (Eq. (3)) in the alternating case is

$$\hat{u}_0(k) = m\sum_{j=1}^{N}(-1)^{j+1}\mathrm{e}^{\mathrm{i}kx_j}, \tag{A.1}$$

$$= m\mathrm{e}^{\mathrm{i}kx_1}\sum_{j=1}^{N}(-1)^{j+1}\mathrm{e}^{\mathrm{i}k(x_j-x_1)}, \tag{A.2}$$

where $\mathrm{i}^2 = -1$. For all j we have $|k(x_j - x_1)| \leq kL$, so that for $kL \ll 1$ the exponential term in Eq. (A.2) can be expanded as

$$\mathrm{e}^{\mathrm{i}k(x_j-x_1)} \simeq 1 + \mathrm{i}k(x_j - x_1) + \mathrm{O}(k^2).$$

The Fourier transform of u_0 therefore reads

$$\hat{u}_0(k) \simeq m\mathrm{e}^{\mathrm{i}kx_1}\left(\sum_{j=1}^{N}(-1)^{j+1} + \mathrm{i}k\sum_{j=1}^{N}(-1)^{j+1}(x_j - x_1)\right) + \mathrm{O}(k^2). \tag{A.3}$$

If N is odd the first sum in Eq. (A.3) is equal to 1, so that the energy spectrum $E_0(k) = L^{-1}|\hat{u}_0(k)|^2$ reads at leading order

$$E_0(k) \sim \frac{m^2}{L}, \quad kL \ll 1.$$

If N is even this sum is equal to 0, and we obtain at leading order

$$E_0(k) \sim \frac{m^2}{L}(kL)^2, \quad kL \ll 1.$$

Appendix B. Calculation of $\overline{q}(r)$ for the Cantor set

We construct a triadic Cantor set by dividing an initial segment of width L in three parts, and by repeating this operation M times on the resulting segments. The Cantor set consists of the points x_i at the boundaries of each segment of the fractal structure. We perform a covering of the points with boxes of width r. The minimum number of boxes needed for this covering is $N_{\text{boxes}} \simeq 2^n$, where $n \in [1, M]$ is the index of the subdivision for which segments have a length of order r, i.e. $3^{-n}L \simeq r$. Note that the number of points per covering box of size r is the same in each box, and is equal to

$$\overline{q}(r) = 2^{M+1-n}.$$

Hence

$$\overline{q}(r) \simeq 2^{M+1}/N_{\text{boxes}}(r) = N/N_{\text{boxes}}(r),$$

where $N = 2^{M+1}$ is the total number of points of the structure, demonstrating the homogeneous fractal property of the Cantor set.

Appendix C. Calculation of $\langle \delta\psi_0^2(r) \rangle$ by statistical method

Here we adapt the statistical method of Vassilicos and Hunt [20] to the calculation of the spectrum of a homogeneous fractal pulse field in the non-alternating case.

In this appendix let us interpret averages $\langle \cdot \rangle$ to mean ensemble averages rather than space averages, in which case, following [20],

$$\langle \delta\psi_0^2(r) \rangle \simeq \sum_q (mq)^2 \times P(q, r), \tag{C.1}$$

where $P(q, r)$ is the probability of having q discontinuity points in a compact segment of size r. The probability $P(q, r)$ is an integral over all situations where discontinuity points are concentrated on a small part of the segment or scattered over the whole segment. This integral is

$$P(q, r) = \int_0^r n_q(l)\, \mathrm{d}l,$$

where $n_q(l)$ is the probability of having exactly q points in a segment of width l, the distance between the first and the last such points being equal to l. Vassilicos [18] has shown that $n_q(l) \sim l^{-D}$ independently of q for homogeneous fractals, so that

$$P(q, r) \sim r^{1-D}. \tag{C.2}$$

Nevertheless, $P(q, r)$ does depend on q, and the dominant contribution to the right-hand side of (C.1) comes from $q = \overline{q}(r)$, so that by using results (16) and (C.2) we get

$$\langle \delta\psi_0^2(r) \rangle \sim r^{D+1}, \tag{C.3}$$

in agreement with (19).

Appendix D. The small-scale energy spectrum

The energy spectrum of u_0 for $k \gg 1/\eta$ can be calculated by applying the method of Moffat [14] and Gilbert [8]. The Fourier transform of the field u_0 given by Eq. (3) is

$$\hat{u}_0(k) = \sum_{j=1}^{N} m_j e^{ikx_j},$$

and $k \gg 1/\eta$ implies that $kx_j \gg kx_{j+1}$ for all j, so that $\hat{u}(k)$ is a sum of N complex numbers with effectively random phases and moduli $|m|$. In the complex plane, this sum can be seen as the result of a random walk with constant steps. The modulus of $\hat{u}_0(k)$ therefore scales like $\sqrt{N}$, and

$$E_0(k) = \frac{1}{L}|\hat{u}_0(k)|^2 \sim \frac{m^2}{L}N \quad \text{for } k \gg 1/\eta,$$

which is the value we obtain in both the alternating and non-alternating cases, for both fractal and spiral distributions of pulses (Eqs. (14), (23) and (42)).

Appendix E. Use of the wavelet transform

In order to avoid high-frequency oscillations in the Fourier transform we make use of the wavelet transorm of $u_0(x)$:

$$\tilde{u}_0(l, b) = \int_{-\infty}^{+\infty} \frac{1}{\sqrt{l}} \phi\left(\frac{x-b}{l}\right) u_0(x)\, dx, \tag{E.1}$$

where ϕ denotes the wavelet, with scale l and position b. We define the wavelet spectrum as (see also [5])

$$E_{\omega 0}(l) = \int_{-\infty}^{+\infty} |\tilde{u}_0(l, b)|^2\, db. \tag{E.2}$$

By Fourier transforming Eq. (E.1) and using the Plancherel identity we get

$$E_{\omega 0}(l) = lL \int_{-\infty}^{+\infty} |\hat{\phi}(lk)|^2 E_0(k)\, dk, \tag{E.3}$$

where $E_0(k) = (1/L)|u_0(k)|^2$ is the Fourier energy spectrum. It follows that when $E_0(k) \sim k^p$ in a range $k_1 \ll k \ll k_2$, we obtain

$$E_{\omega 0}(l) \sim \left(\frac{1}{l}\right)^p \quad \text{for } 1/k_2 \ll l \ll 1/k_1,$$

so that in a log–log plot the slope of the wavelet spectrum is also the slope of the Fourier spectrum. In Fig. 5 and 7 we use the notation $E_{\omega 0}(k)$ with $k = 1/l$ rather than $E_{\omega 0}(l)$ for easiest comparison with $E_0(k)$.

Appendix F. Calculation of $\langle \delta\psi_0^2(r) \rangle$ for spiral non-alternating pulse fields

Let us first note that in the limit where $\eta \ll \alpha L$ we have $N \gg 1$, $\eta \ll x_N$ and $x_N \ll \alpha L$. In this appendix we prove that in the limit $\eta/(\alpha L) \to 0$, $T_2(r) \gg T_1(r)$, $T_3(r)$ in the range $\eta \ll r \ll x_N$ and $T_1(r) \gg T_2(r)$, $T_3(r)$ in the range $x_N \ll r \ll \alpha L$.

The asymptotic limits $T_3(r)/T_2(r) \to 0$ in the range $\eta \ll r \ll x_N$ and $T_3(r)/T_1(r) \to 0$ in the range $x_N \ll r \ll \alpha L$ follow, respectively, from (28) and (33) and from (28) and (36). Use must be made of $N \simeq (\alpha L/\eta)^D$, $D = 1/(\alpha + 1)$ and $\eta \ll \alpha L$.

To show that $T_1(r)/T_2(r) \to 0$ in the range $\eta \ll r \ll x_N$ we start from (34) where we can replace the sum by an integral and obtain (for $\alpha \neq 1, 2$, but the cases $\alpha = 1$ and $\alpha = 2$ can be treated similarly)

$$T_1(r) \simeq \alpha L \left[-\frac{N^{2-\alpha}}{\alpha} + \frac{N^2}{\alpha} n_N^{-\alpha} + \frac{N^{2-\alpha}}{2-\alpha} - \frac{n_N^{2-\alpha}}{2-\alpha} - \frac{2N^{2-\alpha}}{1-\alpha} + \frac{2N}{1-\alpha} n_N^{1-\alpha} \right].$$

When $r \ll x_N$, $n_N \simeq N(1 + \alpha^{-2} r/x_N)$ and therefore

$$T_1(r) = \alpha L N^{2-\alpha} \mathrm{O}\left(\left(\frac{r}{x_N} \right)^3 \right), \tag{F.1}$$

which implies, by using (33), that $T_1(r)/T_2(r) \ll 1$ when $\eta \ll r \ll x_N$.

To show that, when $\eta/(\alpha L) \to 0$, $T_2(r)/T_1(r) \to 0$ in the range $x_N \ll r \ll \alpha L$, we start from (29). The condition $x_N \ll r$ guarantees that I defined by $(r/L) I^\alpha \simeq 1$ is such that $I \ll N$. In fact $I \ll N_c$ because $r \ll \alpha L$. Hence,

$$q(x, r) = i - n_i(r) \simeq i - \left(\frac{r}{L} \right)^{-1/\alpha}, \tag{F.2}$$

and

$$T_2(r) \simeq \alpha L \sum_{i=N_c+1}^{N} i^{1-\alpha} \left(1 - \frac{2}{i} \left(\frac{r}{L} \right)^{-1/\alpha} \right) \quad \text{for } x_N \ll r \ll \alpha L, \tag{F.3}$$

and upon replacing the sum by an integral,

$$T_2(r) \simeq \frac{\alpha L}{2-\alpha} (N^{2-\alpha} - N_c^{2-\alpha}) - \frac{2\alpha L}{1-\alpha} \left(\frac{r}{L} \right)^{-1/\alpha} (N^{1-\alpha} - N_c^{1-\alpha}) \quad \text{for } x_N \ll r \ll \alpha L,$$

where we have assumed $\alpha \neq 1, 2$ (the cases $\alpha = 1$ and $\alpha = 2$ can be dealt with similarly). It then follows using (36) and the conditions $\eta \ll x_N \ll r \ll \alpha L$ that $T_2(r)/T_1(r) \ll 1$ in the range $x_N \ll r \ll \alpha L$.

Appendix G. Asymptotic expansion of energy and correlation length scale

The integrals involved in the calculation of the energy (Eq. (10)) and of the correlation length scale (Eq. (11)) of the linear diffusion problem (Section 3) can be written in terms of the incomplete gamma function. Indeed, these integrals are of the form

$$I = \int_{1/l_1}^{1/l_2} k^{\beta} \mathrm{e}^{-2\nu k^2 t},$$

where l_1 and l_2 are characteristic scales of the structure, and β depends on D. By performing the change of variables $y = 2\nu k^2 t$ we get

$$I = \frac{1}{2}(2\nu t)^{-(\beta+1)/2} \int_{2\nu t/l_1^2}^{2\nu t/l_2^2} y^{(\beta+1)/2-1} \mathrm{e}^{-y}\, \mathrm{d}y,$$

which can be written

$$I = \frac{1}{2}(2\nu t)^{-(\beta+1)/2} \left[\Gamma\left(\frac{\beta+1}{2}, \frac{2\nu t}{l_1^2}\right) - \Gamma\left(\frac{\beta+1}{2}, \frac{2\nu t}{l_2^2}\right) \right],$$

where $\Gamma(\alpha, x)$ denotes the incomplete gamma function. In all cases the time t is such that $\nu t/l_1^2 \ll 1 \ll \nu t/l_2^2$, so that the gamma functions in the above equation can be expanded as (see [1])

$$\Gamma(\alpha, x) = \Gamma(\alpha) - x^{\alpha}/\alpha + \mathrm{O}(x^{\alpha+1}), \quad x \to 0, \tag{G.1}$$

and

$$\Gamma(\alpha, x) = x^{\alpha-1}\mathrm{e}^{-x}(1 + \mathrm{O}(1/x)), \quad x \to +\infty.$$

The asymptotic development (G.1) is valid for $\alpha \neq 0, -1, -2, \ldots$, which is the case in all our calculations, except in Section 3.2.2 where $\beta = -1$, so that $\alpha = 0$. In Section 3.2.2 we expand the gamma function as

$$\Gamma(0, x) = -\gamma - \ln(x) + \mathrm{O}(x), \quad x \to 0,$$

where $\gamma \simeq 0.577$ is Euler's constant.

References

[1] Abramowitz, Stegun, Handbook of Mathematical Functions, Dover, New York, 1965.
[2] E.R. Benton, G.W. Platzman, A table of solutions of the one-dimensional Burgers equation, Q. Appl. Math. 30 (1972) 195–212.
[3] J.M. Burgers, The Nonlinear Diffusion Equation, Reidel, Dordrecht, 1974.
[4] D. Cole, On a quasi-linear parabolic equation occuring in aerodynamics, Q. Appl. Math. 9 (1951) 225.
[5] M. Farge, Wavelet transforms and their applications to turbulence, Ann. Rev. Fluid Mech. 24 (1992) 395–457.
[6] P. Flohr, J.C. Vassilicos, Accelerated scalar dissipation in a vortex, J. Fluid Mech. 348 (1997) 295–317.
[7] J.D. Fournier, U. Frisch, L'équation de Burgers déterministe et statistique, Journal de Mécanique Théorique et Appliquée 2 (5) (1983) 699–750.
[8] A. Gilbert, Spiral structures and spectra in two-dimensional turbulence, J. Fluid Mech. 193 (1988) 475–497.
[9] S.N. Gurbatov, D.G. Crighton, The nonlinear decay of complex signals in dissipative media, Chaos 5 (3) (1995) 524–530.
[10] H.G.E. Hentschel , I. Procaccia, The infinite number of dimensions of probabilistic fractals and strange attractors, Physica D (1983) 435.
[11] E. Hopf, The partial differential equation $u_t + uu_x = u_{xx}$, Commun. Pure Appl. Math. 3 (201) (1950).
[12] S. Kida, Asymptotic properties of Burgers turbulence, J. Fluid Mech. 93 (1979) 337–377.
[13] T.S. Lundgren, Strained spiral vortex model for turbulent fine structure, Phys. Fluids (1982) 25.
[14] H.K. Moffatt, Simple topological aspects of turbulent vorticity dynamics, in: Tatsumi (Ed.), Proceedings IUTAM Symposium on Turbulence and Chaotic Phenomena in Fluids, 1984, p. 223.
[15] F. Nicolleau, J.C. Vassilicos, Intermittency and wavelet analysis of one-point turbulence data (1998), submitted.

[16] P.L. Sachdev, Nonlinear Diffusive Waves, Cambridge University Press, Cambridge, 1987.
[17] T. Tatsumi, S. Kida, Statistical mechanics of the Burgers model of turbulence, J. Fluid Mech. 55 (1972) 659–675.
[18] J.C. Vassilicos, The multispiral model of turbulence and intermittency, in: H.K. Moffatt et al. (Eds.), Topological Aspects of the Dynamics of Fluids and Plasmas, 1992, pp. 427–442.
[19] J.C. Vassilicos, Anomalous diffusion of isolated flow singularities and of fractal or spiral structures, Phys. Rev. E 52 (6) (1995).
[20] J.C. Vassilicos, J.C.R. Hunt, Fractal dimensions and spectra of interfaces with application to turbulence, Proc. Roy. Soc. Lond. A 435 (1991) 505.